

MIDDLE MIOCENE GLOBAL CHANGE AND PALEO GEOGRAPHY OF PANAMA

GREGORY J. RETALLACK^{1*} and MICHAEL XAVIER KIRBY²

¹Department of Geological Sciences, University of Oregon, Eugene, Oregon 97403, USA; ²Center for Tropical Paleocology and Archeology, Smithsonian Tropical Research Institute, Box 2072, Balboa, Republic of Panama
e-mail: gregr@uoregon.edu

ABSTRACT

Fossil leaves in the middle Miocene Cucaracha Formation along the Panama Canal are 10–15 cm long, thick, and entire-margined; fossil pollen is also dicot dominated, as expected for wet tropical forests. Fossil woods include palms and ring-porous dicots, with smooth bark as is found in weakly seasonal tropical climates. In contrast, late Hemingfordian to early Barstovian mammals of the Cucaracha Formation are the same as those found in Nebraska, Kansas, and Florida, where climate was drier and cooler and vegetation more open. Cucaracha paleosols reconcile these differences as evidence of a mosaic of swamps to mangal (mangrove forests) preserving plants and dry uplands preserving mammals. A dozen pedotypes represent as many vegetation types, including mangrove, fresh-water and marine-influenced swamp, early successional riparian woodland, colonizing forest, dry tropical forest, and woodland. Many paleosols have calcareous nodules, and some have pedogenic barite nodules. Depth to carbonate and paleosol thickness with carbonate indicate mean annual precipitation of $573\text{--}916 \pm 147$ mm and mean annual range of precipitation of $27\text{--}65 \pm 22$ mm. Chemical analyses of paleosol Bt horizons confirm mean annual precipitation of 296–1142 mm and mean annual temperature of $15\text{--}16 \pm 4.4^\circ\text{C}$. Low precipitation and temperature estimates imply a rain shadow from a high (1400–4000 m) volcanic mountain range to the west, with continuous land connection to allow immigration of mammals from North America. Partial enclosure of the Caribbean Sea by a mountainous Panama peninsula, as well as by Antillean arcs, initiated high Caribbean marine temperature and salinity well before Pliocene isthmian closure.

INTRODUCTION

The middle Miocene Cucaracha Formation of Panama has yielded plant remains of wet neotropical forests (Berry, 1981; Graham, 1988a, 1988b) as well as fossil mammals also known from the semiarid Great Plains of North America (Kirby and MacFadden, 2005). Here we use evidence from paleosols to arbitrate this discrepancy and to further illuminate middle Miocene climate and vegetation of Panama and the role of peninsular-to-isthmian constriction in global paleoclimatic change.

Panama played an important role as a Cenozoic barrier to marine and atmospheric circulation (Bartoli et al., 2005) and as a corridor of inter-hemispheric biotic exchange (Webb and Rancy, 1996). Panama during the middle Miocene has been interpreted as an archipelago until 2.74–3.15 Ma (Coates and Obando, 1996; Coates et al., 2004; Bartoli et al., 2005), when a land bridge allowed plant and mammal interchange between North and South America (Webb and Rancy, 1996) and separated Caribbean and Pacific marine organisms (Marincovich, 2000).

Completion of the land bridge has been considered a tipping point in Cenozoic global climate deterioration and ocean current reorganization at the onset of northern hemisphere Pleistocene glaciation (Lear et al., 2003). The Caribbean Sea is currently 2°C warmer and 1.5 ‰ more

saline, with less marked seasonal upwelling than the Pacific Ocean (Broecker, 1989). The Caribbean Sea supplies warm saline water to the Gulf Stream and to North Atlantic deep-water formation, which in turn drives global thermohaline circulation (Curry et al., 2006). Panama isthmus closure would have driven warm saline waters to higher latitudes at 3.15–2.74 Ma (Cronin and Dowsett, 1996; Bartoli et al., 2005). Key components of this argument were dating Panamanian isthmus closure to the onset of northern Atlantic cooling between 2.0 Ma and 1.8 Ma and linking a warmer, stronger Gulf Stream to North Atlantic glaciation (Broecker, 1989). Unfortunately, a date of 3.1–2.8 Ma for closure coincides with global marine warming (Zachos et al., 2001) that occurred when a warmer North Atlantic and a stronger Gulf Stream melted glaciers and icebergs instead of bringing on glaciation (Retallack, 2002; Lund et al., 2006).

An alternative view is that Central America was a long peninsula by 16 Ma, with the exception of a narrow marine passage between Panama and Colombia, considering the close similarity of middle Miocene Panamanian fossil mammals to those of North America (Whitmore and Stewart, 1965; Kirby and MacFadden, 2005; MacFadden, 2006). Isotopic profiles through growth zones of late Miocene (10.2–5 Ma) marine clams in northwest Panama indicate warm, weakly seasonal waters more like the modern Caribbean than Pacific Ocean (Teranes et al., 1996). In addition, a greater Antillean landmass restricted Caribbean circulation as long ago as 32 Ma (Iturralde-Vinent and MacPhee, 1999). Palynofloras indicate also that early-middle Miocene Panama included highlands with pre-montane rain forest now found at elevations of as much as 1400 m (Graham, 1982, 1988a, 1988b, 1989). Narrowing of the oceanic connection and restriction of cool, low-salinity Pacific waters into the Caribbean at the Oligocene-Miocene boundary has been implicated in early Miocene coral extinctions (von der Heydt and Dijkstra, 2005). The middle Miocene was a time of globally warm temperatures at 16 Ma, followed at 15 Ma by cooling and drying (Zachos et al. 2001; Retallack 2002).

Did Caribbean enclosure play a role in middle Miocene global warming long before the late Pliocene? Or were other global causes more important: Himalayan uplift (Raymo and Ruddiman, 1992), grass-grazer coevolution (Retallack, 2001b), volcanism (McBirney et al., 1974), or meteorite impact (Dressler and Reimold, 2001)?

GEOLOGICAL SETTING AND AGE

The Cucaracha Formation is the continental volcanoclastic upper part of the Gaillard Group (Figs. 1–2). The best age indicators for the Cucaracha Formation are its fossil mammals (Table 1), which include seven species known from the late Hemingfordian and early Barstovian of North America (MacFadden and Higgins, 2004; MacFadden, 2006), dated at 16 ± 1.5 Ma, as calibrated by magnetostratigraphy and radiometric dating (Tedford et al., 2004). Two K-Ar dates from a dacitic ash-flow tuff within the Cucaracha Formation of 22.2 ± 1.7 and 18.9 ± 2.2 Ma (Woodring, 1982) are significantly older and differ from each other so much that they cast doubt on their accuracy. The underlying marine Culebra Formation has mollusks correlated with the European Aquitanian (Woodring, 1982), 20.43–23.03 Ma in the time scale of Gradstein et al. (2004), but its benthic foraminifera are like those of the California Saucian (Blacut and

* Corresponding author.

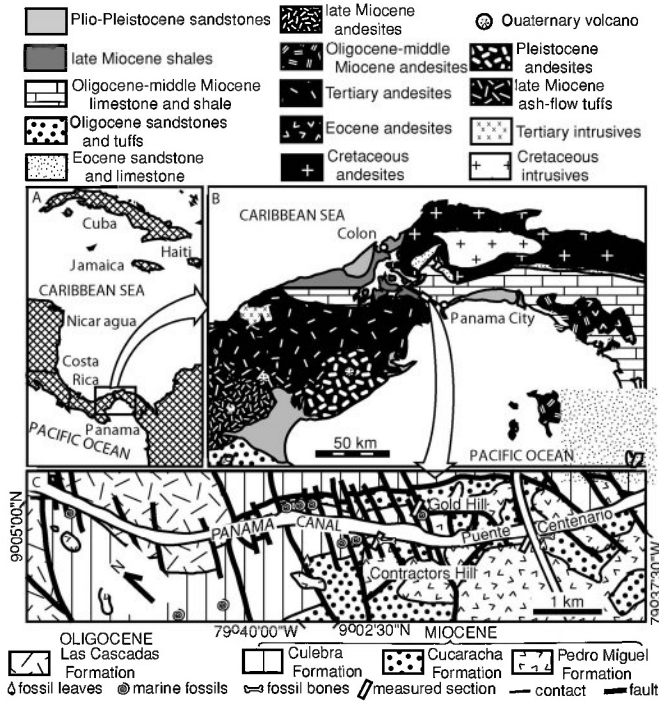


FIGURE 1—Geological map of Panama (after Weyl, 1980) and Panama Canal showing measured sections (after Woodring, 1982).

Kleinpell, 1969), currently dated 24–17 Ma (Prothero, 2001). Ostracodes from the Culebra Formation (Bold, 1973) indicate correlation with planktonic foraminifer zone N6 (Blow, 1969), which is 17.4–17.5 Ma in the time scale of Gradstein et al. (2004). An early Miocene age is compatible with the 31 coral species in the Emperador Limestone Member of the Culebra Formation (Johnson and Kirby, 2006). Only two species of fossil wood were described from the Cucaracha Formation by Berry (1918). His three sites for fossil leaves (near station 1760, 0.4 km south of Gaillard Group of Empire Bridge and below Miraflores Locks) were formerly regarded as Culebra Formation and Oligocene to early Miocene but are now mapped in the Cucaracha Formation (Woodring, 1982). Palynofloras of the Cucaracha Formation from coal and carbonaceous shale of the Panamanian Puente Centenario section have been studied for paleoecology but not age (Graham, 1988b).

MATERIALS AND METHODS

Three long sections of paleosols were measured in the Cucaracha Formation (Fig. 3): 1) Panama Canal western shore up the slope beneath the southwestern footing of the new Puente Centenario bridge (N9.03060°, W79.63502°), 2) east-facing slopes above the track north of Contractors Hill (N9.04560°, W79.65079°), and 3) recent excavations on north-facing slopes of Gold Hill (N9.04451°, W79.64263°). Different paleosols were classified into pedotypes (Tables 2–3) and named for characteristic features in the native Embera language (Binder and Ismarg, 1997). Type sections for each pedotype were logged in greater detail (Fig. 4). Special care was taken to measure with a milliner's tape three variables of the carbonate horizons of these paleosols as guides to paleoclimate and duration of soil formation (Retallack, 2005): depth of nodules from the surface of the paleosol, thickness of paleosol with nodules, and average size of nodules visible in outcrop. These paleosols were then classified in order to find analogous modern soils using three modern soil classifications: the U.S. soil taxonomy (Soil Survey Staff, 1999), the classification of the Food and Agriculture Organization World Soil Map (Food and Agriculture Organization, 1974), and the Australian classification (Isbell, 1996).

Petrographic thin sections of barite nodules, fossil wood, and rhizoliths were prepared (specimens are curated in the Condon Museum Collection,

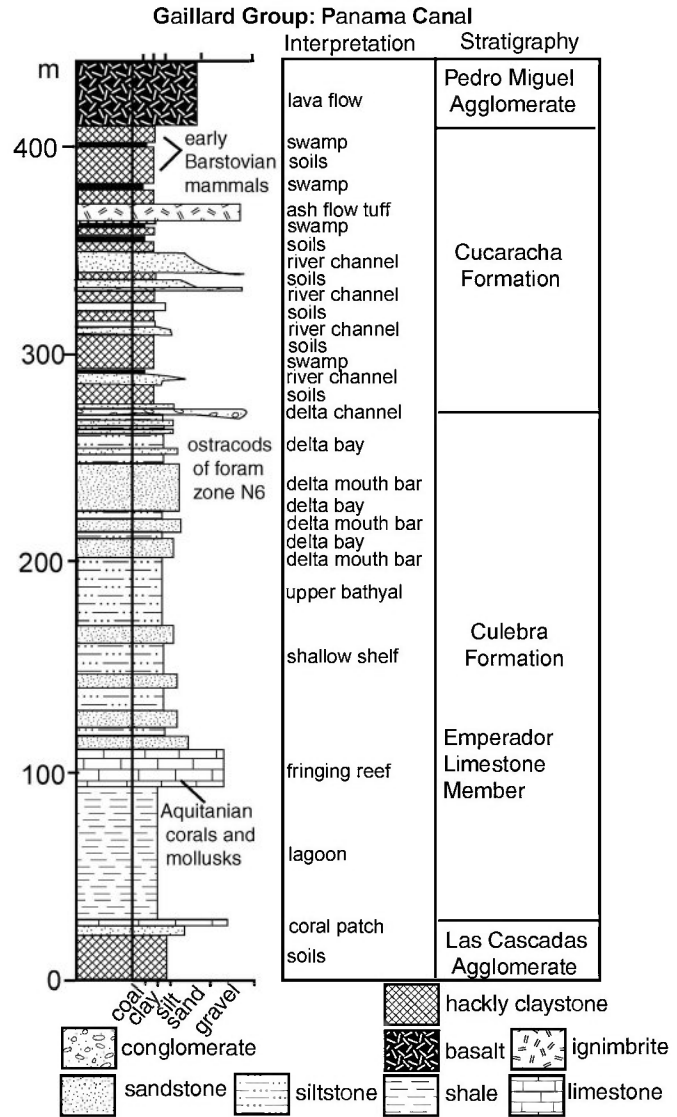


FIGURE 2—Stratigraphy and paleoenvironments of the Miocene Gaillard Group, Panama.

University of Oregon, Eugene). Barite nodules and paleosol samples were analyzed by R.K. Rogers of ALS Chemex in Sparks, Nevada, using X-ray fluorescence for major element chemical composition, including total Fe as Fe₂O₃. Errors were calculated from 10 replicates of the laboratory standard. Rare earth elements (REE) were determined by using instrumental neutron activation analysis, performed by L.D. Minc of the Oregon State University Radiation Center, Corvallis, using a coal fly ash standard (NIST1633a; U.S. National Institute of Standards and Technology). The instrumental neutron activation analysis data came from 7 h radiation on a rotating track, with an average thermal flux of 10¹² n·cm⁻²·s⁻¹. Two separate counts of gamma decays were made: one after a 5-day decay for 5000 seconds, and another after 4-week decay of 10,000 seconds. Errors shown in Table 4 are averages of individual count errors for that element. Unusually high barite increased the background of the instrumental neutron activation analysis results, leading to compromised detection of Lu, Ce, Sm, and Yb in two of the samples (R3195 and R3196).

PALEOENVIRONMENTS

Characterization of the paleoenvironments of the Cucaracha Formation, which have been interpreted from sedimentology and invertebrate paleontology as a tropical coastal sequence formed at a time of locally low

TABLE 1—Fossils from the Cucaracha Formation.

Taxon	Reference	Comment
<i>Selaginella</i> sp. indet.	Graham, 1988b	Herbaceous lycopsid
Filicales sp. indet. type 1	Graham, 1988b	Monolete fern spore
Filicales sp. indet. type 2	Graham, 1988b	Monolete fern spore
Filicales sp. indet. type 3	Graham, 1988b	Monolete fern spore
Filicales sp. indet. type 4	Graham, 1988b	Monolete fern spore
<i>Cyathea</i> sp. indet.	Graham, 1988b	Tree fern spores
<i>Acrostichum</i> sp. indet.	Berry, 1918	Mangrove fern fragments
<i>Ceratopteris</i> sp. indet.	Graham, 1988b	Floating fern spores
<i>Pteris</i> sp. indet.	Graham, 1988b	Tree fern spores
Filicales sp. indet. type 1	Graham, 1988b	Trilete fern spores
Filicales sp. indet. type 2	Graham, 1988b	Trilete fern spores
<i>Cryosophila</i> -type	Graham, 1988b	Rootspine fan palm pollen
<i>Manicaria</i> -type	Graham, 1988b	Pinnate palm pollen
<i>Palmoxylon palmacites</i>	Berry, 1918	Palm wood
" <i>Ficus</i> " <i>culebrensis</i>	Berry, 1918	Evergreen tree (Moraceae) leaf
" <i>Guatteria</i> " <i>culebrensis</i>	Berry, 1918	Evergreen tree (Anonaceae) leaf
<i>Myristicophyllum panamense</i>	Berry, 1918	Evergreen tree (Myristicaceae) leaf
" <i>Mespilodaphne</i> " <i>culebrensis</i>	Berry, 1918	Evergreen tree (Lauraceae) leaf
<i>Melastomites miconioides</i>	Berry, 1918	Evergreen tree (Melastomataceae) leaf
<i>Ilex</i> sp. indet.	Graham, 1988b	Holly (Aquifoliaceae) pollen
Asteraceae sp. indet.	Graham, 1988b	Pollen
<i>Alchornea</i> sp. indet.	Graham, 1988b	Evergreen tree (Euphorbiaceae) pollen
<i>Alfaroa-Engelhardia</i> sp. indet.	Graham, 1988b	Deciduous tree (Juglandaceae) pollen
" <i>Inga</i> " <i>oligocaenica</i>	Berry, 1918	Evergreen tree (Mimosaceae) leaf
" <i>Cassia</i> " <i>culebrensis</i>	Berry, 1918	Evergreen tree (Caesalpinoideae) leaf
<i>Crudia</i> sp. indet.	Graham, 1988b	Evergreen tree (Caesalpinoideae) pollen
<i>Eugenia-Myrica</i> sp. indet.	Graham, 1988b	Evergreen shrub-tree (Myrtaceae) pollen
<i>Rhizophora</i> sp. indet.	Graham, 1988b	Red mangrove (Rhizophoraceae) pollen
<i>Avicennia</i> sp. indet.	Herein	Black mangrove root
<i>Taenioxylon multiradiatum</i>	Berry, 1918	Dicot wood (Fabaceae)
<i>Anadara</i> sp. indet.	Woodring, 1982	Marine cockle
Lucinidae	Woodring, 1982	Marine lucina clam
<i>Tellina (Eurytellina) ophiaca</i>	Woodring, 1982	Marine sunset clam
<i>Hemisinus (Longiverena)</i> aff. <i>H. oeciscus</i>	Woodring, 1982	Freshwater snail
Unionidae	Woodring, 1982	Freshwater clam
<i>Texomys stewarti</i>	MacFadden and Higgins, 2004	Pocket gopher
<i>Tomarcus brevirostris</i>	MacFadden and Higgins, 2004	Early dog
Amphicyonidae-Hemicyonidae	MacFadden and Higgins, 2004	Extinct bear dog
<i>Cynorca</i> sp.	Kirby and MacFadden, 2005	Extinct peccary
<i>Merycochoerus matthewi</i>	MacFadden and Higgins, 2004	Piglike oreodon
<i>Paratoceras wardi</i>	MacFadden and Higgins, 2004	Small protoceratid cameloid
<i>Anchitherium clarenci</i>	MacFadden and Higgins, 2004	Large browsing horse
<i>Archaeohippus</i> sp. indet.	MacFadden and Higgins, 2004	Small browsing horse
<i>Menoceras barbouri</i>	MacFadden and Higgins, 2004	Small two-horn rhinoceros
<i>Floridaceras whitei</i>	MacFadden and Higgins, 2004	Large rhinoceros

sea level and active volcanism (Woodring, 1982; Johnson and Kirby, 2006), can now be augmented with observations from paleosols. A dozen kinds of paleosols (Tables 2–3) represent at least as many past sedimentary subenvironments and vegetation types. The Cucaracha Formation was deposited in a coastal plain flanking the active Chorotega Volcanic Arc to the west (Weyl, 1980), which provided volcanic ash, now weathered to smectite within the paleosols, as well as basalt flows and a dacitic, welded ash-flow tuff. Basalt-pebble conglomerates indicate rugged volcanic-source terranes nearby. A 1.5-km-diameter impact crater near Gamboa, 11 km north of our sites, is K-Ar dated at 41.1 ± 1.3 Ma (Eocene; Tornabene et al., 1999). This would have been covered and disrupted by the caldera source of the welded tuff in the Miocene Cucaracha Formation. High elevations (1400 m) nearby are also suggested by premontane rain-forest pollen of *Engelhardia-Alfaroa* in the Cucaracha Formation (Graham, 1988b).

A coastal setting is indicated by paleosols with abundant pyrite (Dote, Kidua, and Itarra pedotypes) and rhizoliths that are interpreted as peg roots (Fig. 5); these are similar to the intertidal mangrove soils of Florida, United States (Altschuler et al., 1983). Other paleosols are drab with unoxidized Fe but lack pyrite (Chibigi and Paima pedotypes), as is found in fresh-water swamps. Yet others are red and oxidized, owing to good

drainage of the upper meter of the soil (Beredeta, Borobari, Pura and Puriho pedotypes), as is found on the levees and floodplains of Louisiana, United States (Coleman, 1988). All red paleosols have drab-haloed rhizoliths, with the green-from-the-top topology of burial gleization (Retallack, 2000), which is distinct from groundwater gleization envisaged for swampy gray and coaly paleosols and have such additional gley features as pyrite (oxidized to jarosite in outcrop) and siderite nodules (oxidized to high chroma mottles in modern outcrop). Red pedotypes (Beredeta, Borobari, Pura, and Puriho) show drab colors at depth and are interbedded with intermittently gleyed to coaly pedotypes (Chibigi, Dote, Kida, Itarra, and Paima), so they were not formed more than a few meters above the water table. Abundant rhizoliths and some coals, indicating ancient vegetation of high productivity, allowed clear delineation of paleosols, including very weakly developed paleosols (Dume, Epedeko, and Kidua pedotypes), which lacked cumulic surficial additions expected in such lowland paleosol sequences.

A volcanically and tectonically active environment is suggested by abundant weakly developed paleosols (Dume, Epedeko, and Kidua pedotypes), with relict bedding and lacking carbonate nodules and illuviated clay skins of other pedotypes. Moderately developed calcareous paleosols (Chibigi, Beredeta, Borobari, and Puriho pedotypes) have nodules mostly

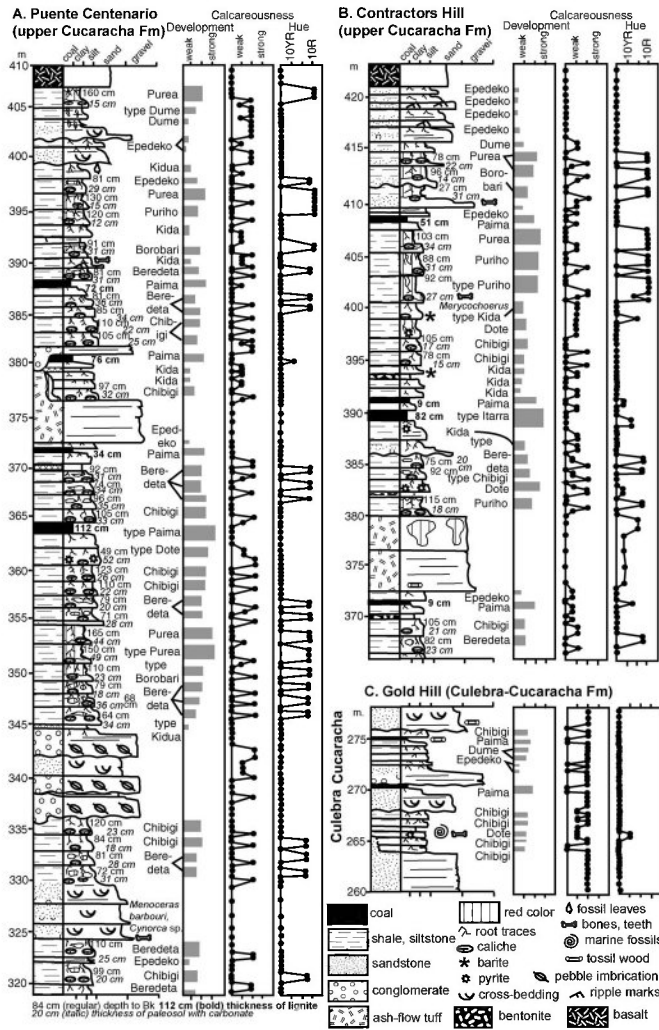


FIGURE 3—Paleosols in measured sections of the Cucaracha Formation. A) Puente Centenario (upper Cucaracha Formation). B) Contractors Hill (upper Cucaracha Formation). C) Gold Hill (Culebra-Cucaracha Formation). Fm = Formation.

less than 2 cm diameter. Nodules of that size take less than 4900 ± 1800 years to form, using a transfer function based on modern soils of New Mexico (Retallack, 2005). The accumulation of woody peats like those of the Cucaracha Formation is also constrained to a rate of about 0.5–1 mm per year because at slower rates plant debris decays rather than accumulates, and at faster rates roots of swamp trees suffocate in stagnant water and curtail the supply of debris (Retallack, 2001a). Using this information to calculate a duration of lignite formation requires adjustment for compaction during overburden, estimated to at about 800 m above the Cucaracha Formation (Woodring, 1957). Under those conditions modern Histosols would be compacted to a quarter of their original thickness (Sheldon and Retallack, 2001), and the lignites of the Cucaracha Formation now 9–112 cm thick took some 364–9064 years to form. Using these and other estimates of the different pedotype durations (Table 3), we get a rock accumulation rate for the Puente Centenario section of $0.19 \text{ mm}\cdot\text{y}^{-1}$ and of the Contractors Hill section of $0.15 \text{ mm}\cdot\text{y}^{-1}$. This is comparable with $0.22 \text{ mm}\cdot\text{y}^{-1}$ computed from early Oligocene volcanoclastic paleosols of Oregon back-arc basins (Retallack, 1998). It is also comparable with long-term rates computed from radiometric dating of $0.19 \text{ mm}\cdot\text{y}^{-1}$ for 695 m of volcanoclastic sediment at 37 Ma in Nebraska (Schultz and Stout, 1980) but is less than $0.50 \text{ mm}\cdot\text{y}^{-1}$ for intermontane Montana with 2240 m since 45 Ma (Hanneman and Wideman, 1991) or $0.65 \text{ mm}\cdot\text{y}^{-1}$ for back-arc basins in Oregon with 2850 m since 45 Ma (Retallack et al., 2000).

PEDOGENIC BARITE?

Barite nodules, which appear to be part of the genetic profile of the Kida pedotype, are a puzzling aspect of the middle Miocene paleosols of Panama. They form a distinct horizon within these paleosols in bedded silts below the surface horizon of rooting. Barite forms spherules with thin radiating crystals and a honeycomb-like pattern of ridges on the surface (Figs. 6A–B) reminiscent of the barite desert roses of Oklahoma, Wyoming, South Africa, and Egypt (Table 5). Barite also forms nodules with randomly arrayed barite laths and a granular surface (Figs. 6D–E). Both the spherules and nodules include quartz and other grains from the matrix (Figs. 6C–F), and they also show evidence of bedding planes and lateral linkage (Fig. 6D). These are indications that barite replaced pre-existing matrix in a manner comparable to that of pedogenic carbonate (Retallack, 1983).

Barite in soils and sediments can be present as weather-resistant clasts from barite-bearing bedrock, but in that case it maintains the clear crys-

TABLE 2—Pedotypes of the Cucaracha Formation.

Pedotype	Embera meaning (Binder and Ismare, 1977)	Diagnosis	US Soil Taxonomy (Soil Survey Staff 1999)	World Map (FAO, 1974)	Australian Handbook (Isbell, 1996)
Beredeta	Black-red bean necklace	Gray-purple mottled siltstone (A) over calcareous nodules (Bk)	Endoaquept	Calcaric Gleysol	Redoxic Hydrosol
Borobari	Crown	Gray green silty surface (A) over mottled green and red (I0R) silty (Bw) and calcareous nodules (Bk)	Aquic Calcicustept	Calcic Cambisol	Calcenic Tenosol
Chibigi	Turtle	Gray siltstone (A) over calcareous nodules (Bk)	Humaquept	Calcaric Gleysol	Oxyaquic Hydrosol
Dote	Pole	Pyritic-jarositic claystone (A) over calcareous nodules (Bk)	Sulfaquept	Thionic Fluvisol	Intertidal Hydrosol
Dume	Notched log ladder	Gray siltstone (A) over siltstone (Bw) with abundant calcareous rhizoconcretions	Ustifluent	Calcaric Fluvisol	Supra-calcic Calcarosol
Epedeko	Plate	Gray rooted and bedded shale (A)	Fluvaquent	Eutric Fluvisol	Stratic Rudosol
Itarra	Fire hearth	Thick pyritic-jarositic coal (O) and gray underclay (A)	Sulfhemist	Dystric Histosol	Hemic Organosol
Kida	Tooth necklace	Gray siltstone (A) over siltstone (C)	Fluvaquent	Eutric Fluvisol	Grey-Orthic Tenosol
Kidua	Leaves	Pyritic-jarositic rooted and bedded shale (A)	Sulfaquept	Thionic Fluvisol	Intertidal Hydrosol
Paima	Black	Thick coal (O) over noncalcareous gray claystone (A)	Haplofibrist	Dystric Histosol	Fibric Organosol
Purea	Red	Gray green clayey surface (A) over thick (1 m), red (I0R) clayey (Bt) horizon.	Haplustalf	Calcic Cambisol	Red Dermosol
Puriho	Guava	Gray green silty surface (A) over red, clayey (Bt) and calcareous nodules (Bk)	Typic Calcicustept	Calcic Luvisol	Red Dermosol

TABLE 3—Interpreted pedotypes of the Cucaracha Formation. MAP = mean annual precipitation; MARP = mean annual range of precipitation.

Pedotype	Climate	Organisms and ecosystems	Topography	Parent material	Time to form
Beredeta	Subhumid (573–784 mm MAP), weakly seasonal (31–48 mm MARP)	Seasonally dry lowland forest with <i>Menoceras barbouri</i> , <i>Cynorca</i> sp.	Floodplain depression	Alluvial silt	2–6 kyr
Borobari	Subhumid (703–782 mm MAP), weakly seasonal (37–44 mm MARP)	Dry pole woodland, with <i>Mery-cochoerus matthewi</i>	Low alluvial terrace	Rhyodacitic volcanic ash	4–8 kyr
Chibigi	Subhumid (643–824 mm MAP), weakly seasonal (29–48 mm MARP)	Lowland forest, turtle	Floodplain depression	Alluvial silt	2–6 kyr
Dote	Subhumid (486–639 mm MAP), weakly seasonal (40–65 mm MARP)	Mangal, with <i>Avicennia</i>	Intertidal, wave protected	Alluvial and marine silt	2–4 kyr
Dume	Not diagnostic for climate	Littoral woodland	Coast and lake beach	Alluvial-eolian silt	0.2–0.8 kyr
Epedeko	Not diagnostic for climate	Riparian early successional	Streamside swale	Alluvial silt	0.005–0.1 kyr
Itarra	Not diagnostic for climate	Back mangal	Coastal depression	Alluvial silt	3.3–6.6 kyr
Kida	Not diagnostic for climate	Riparian early successional, with turtle, <i>Parotoceras wardi</i> , <i>Menoceras barbouri</i>	Streamside swale and levee	Rhyodacitic volcanic ash	0.05–0.1 kyr
Kidua	Not diagnostic for climate	Back mangal, with palm, dicot, snail (<i>Viviparus</i>)	Estuarine flats	Alluvial silt	0.005–0.1 kyr
Paima	Not diagnostic for climate	Freshwater swamp with palm and dicot wood	Floodplain depression	Alluvial silt	0.36–9.0 kyr
Purea	Humid (641–916 mm MAP) weakly seasonal (28–62 mm MARP)	Dry forest	Well-drained alluvial terrace	Rhyodacitic volcanic ash	5–10 kyr
Puriho	Subhumid (707–842 mm MAP), weakly seasonal (31–40 mm MARP)	Dry woodland	Well-drained alluvial terrace	Rhyodacitic volcanic ash	5–10 kyr

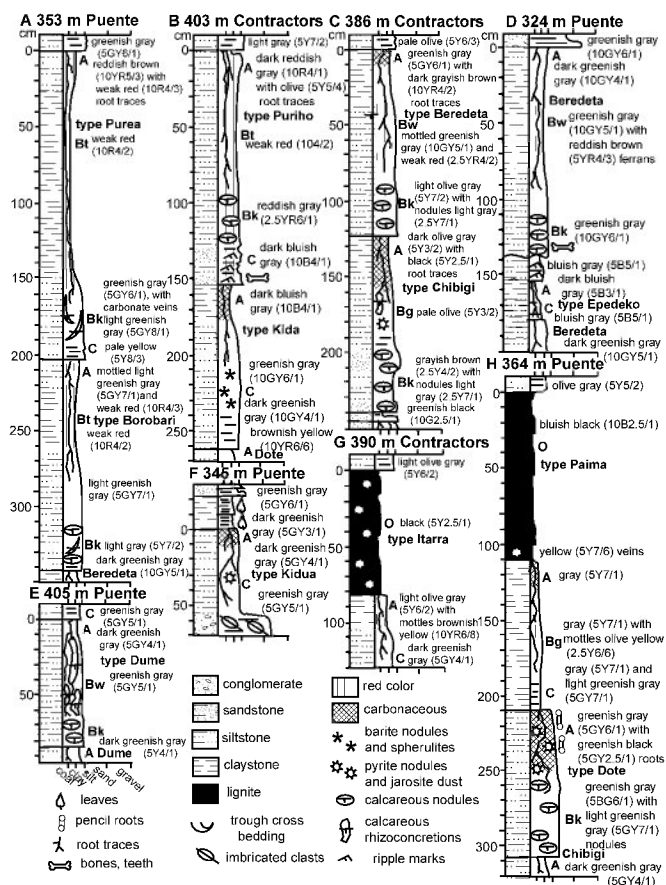


FIGURE 4—Type profiles of pedotypes of the Cucaracha Formation. A) 353 m, Puente. B) 403 m, Contractors. C) 386 m, Contractors. D) 324 m, Puente. E) 405 m, Puente. F) 345 m, Puente. G) 390 m, Contractors. H) 364 m, Puente.

talline form of the parent barite (Lewis, 1923; Robinson et al., 1939; Goosens, 1969; Merefild, 1975). Barite also forms clear crystals in coal cleat or other vugs, precipitated during deep burial (Pe-Piper et al., 2005). This is not the case for opaque crystals of barite with other mineral inclusions in the middle Miocene of Panama or other instances of barite rosettes (Table 5).

Another possibility is that barite nodules and spherulites of the middle Miocene paleosols of Panama were produced by unusual volcanic fluids or tuffs. Water released from the acidic crater lake of Ijen Caldera in Indonesia lost barium downstream, but the barium did not form into recognizable nodules (Delmelle and Bernard, 2004). Carbonatite lavas are a promising source for barite because they are rich in both BaO and SO₃, which are on average, respectively, 0.34 (0–5.0) and 0.88 (0.02–3.87) wt% for calcicarbonatites, 0.64 (0.01–4.30) and 0.69 (0.06–1.5) wt% for magnesiocarbonatites, and 3.25 (0.02–20.60) and 0.88 (0.01–5.95) wt% for ferrocarbonatite (Woolley and Kempe, 1989). Enrichment of light REE is a distinctive signature of carbonatite lavas and tuffs, as are elevated F, Sr, and Nb (Woolley and Kempe, 1989). Carbonatites are thus very distinct from the flat REE profiles of the Panama barites, their matrix, and associated soils (Fig. 7). Enrichment of REE due to weathering is also apparent from our data, which demonstrate a bowl shape. This pattern is caused by light-REE-enrichment due to clay formation and heavy-REE-enrichment due to carbonate in soils (Compton et al., 2003) and paleosols (Metzger et al., 2004). Barite-bearing Kida paleosols did not have a parent material unusual for Cucaracha Formation paleosols.

Barium is rare in modern soils: a systematic survey of 1319 soils in the United States showed a mean concentration of only 440 ± 2 ppm Ba (Shacklette and Boerngen, 1984). Barium sulfate is extremely insoluble (0.0024 g in 100 g of water), as is barium carbonate (0.0023 g in 100 g of water), but barium chloride is more soluble (26.3 g in 100 g of water), so chloride waters are a more likely transporting agent than sulfate waters, which cause rapid precipitation of barite (Tarr, 1933; Hanor, 2000; Huston and Logan, 2004). In intraformational waters below the Gulf of Mexico, barium is most abundant in calcium-rich brines and is inversely correlated with sulfate abundance (MacPherson, 1989). A model in which

TABLE 4—Chemical analyses of barite and paleosols by X-ray fluorescence and instrumental neutron activation analysis.

Element sample	Error $\pm 1\sigma$	Barite spherulite R3195	Barite nodule R3196	Kida C horizon R3197	Puriho Bt horizon R3198	Purea Bt horizon R3199
SiO ₂ %	0.77	2.18	6.78	49.99	53.25	47.09
TiO ₂ %	0.044	0.31	0.40	1.41	1.06	0.88
Al ₂ O ₃ %	0.23	0.82	2.65	18.69	16.56	19.87
Fe ₂ O ₃ %	0.20	0.24	0.82	9.10	8.50	10.21
CaO %	0.04	1.72	0.23	1.53	1.75	1.63
MgO %	0.04	0.08	0.13	0.91	0.90	1.16
Na ₂ O %	0.05	0.93	0.90	0.60	0.77	0.61
K ₂ O %	0.02	0.04	0.04	0.13	0.33	0.51
Cr ₂ O ₃ %	0.01	0.09	0.04	0.02	0.01	0.01
MnO %	0.01	0.20	0.04	0.02	0.02	0.02
P ₂ O ₅ %	0.015	0.04	0.04	0.02	0.08	0.06
SrO %	0.003	0.4	0.40	0.04	0.05	0.05
BaO %	0.05	69.76	65.43	0.14	0.10	0.03
LOI %	—	1.92	4.14	17.10	16.35	17.60
TOTAL	—	79.01	82.04	99.71	99.73	99.72
La ppm	0.71	2.96	2.25	8.53	13.02	36.26
Nd ppm	2.8	<15	<14	<15	<15	37.58
Sm ppm	0.19	0.38	0.36	1.21	3.71	10.78
Yb ppm	0.13	<0.43	<0.40	0.71	2.92	5.16
Lu ppb	31.2	<95	<90	135	435	753

calcic chloride brines meet sulfate waters caused by oxidation of pyrite would precipitate barite (Torres et al., 1996) is compatible with the coastal setting of the Panamanian paleosols, which include acid-sulfate mangal (mangrove swamp) paleosols (Itarra and Dume pedotypes).

The main problem with this scenario is that large (>15 μm) barite spherulites and nodules have not been recorded in these soils, even though they are locally common in paleosols (Table 5). Microscopic ($2 \times 15 \mu\text{m}$) needles of barite line ped faces in the lower B and upper C horizons of well-developed soils, including Ultisols (Stoops and Zavaleta, 1978), Alfisols (Carson et al., 1982; Darmody et al., 1989), and Mollisols (Lynn et al., 1971). They have been attributed to precipitation from saline groundwater (Stoops and Zavaleta, 1978) and to local effects of acid-sulfate weathering (Carson et al., 1982). Intracellular, 1–4- μm -diameter barite spherules and nodules are formed by many microbes (Hanor, 2000; González-Muñoz et al., 2003): marine coccolithophorids (*Exanthemachrysis*), foraminifera (*Hyperammina*) and xenophyophores (*Occultammina*); soil and marine myxobacteria (*Myxococcus*); and fresh-water desmids (*Closterium*) and ciliophorans (*Loxodes*). These dustings in soils and within microorganisms are much smaller than the >1-cm-diameter barite nodules and spherulites in paleosols of Panama and elsewhere (Table 5).

Geologically unusual conditions for pedogenic barite nodule formation are suggested by comparing their known occurrences (Table 5) with the presence of gypsum in paleosols (Table 6). Both barite and gypsum form rosette-shaped sand crystals known as desert roses, but whereas barite forms in paleosols during times of high atmospheric CO₂, which we infer from stomatal index studies (Retallack, 2002), gypsum forms during times of low CO₂, including the present day. Perhaps unusual, chemically aggressive soil waters formed during rainfall in arid lands during such global greenhouse spikes as the middle Miocene (Retallack, 2002). Alternatively, widespread waterlogging and anoxia in soils during such greenhouse spikes as the Permian-Triassic boundary (Sheldon and Retallack, 2002) may have accelerated bioaccumulation of barite by soil myxobacteria. Yet another possibility is a broadcast of barite with a massive methane clathrate outburst, which has been implicated in some atmospheric CO₂ spikes, because oceanic barite increased dramatically in abundance during the Paleocene–Eocene thermal maximum and atmospheric redox crisis (Dickens et al., 2003). Similarly, oceans now are sulfur rich and chemically oxidizing, but before 3.2 Ga marine barite was more abundant and oceans were sulfur poor and chemically reducing (Huston and Logan, 2004). Another contributor to barite precipitation may have been oxidation of sulfides degassed from anoxic oceans during

greenhouse spikes, as proposed for the Permian-Triassic boundary (Kump et al. 2005). Barite spherulites, nodules, and desert roses in paleosols are unusual and may call for unusual conditions of formation.

PALEOCLIMATE

Divergent indicators of humid climate from fossil leaves (Berry, 1918) and pollen (Graham, 1988b) and dry climate from fossil mammals (MacFadden and Higgins, 2004) can be reconciled with evidence from paleosols using two lines of evidence: identification of analogous modern soils (Table 3) and measurement of climate-sensitive paleosol features (Fig. 8). Two climate-sensitive variables were measured for each paleosol: depth to Bk horizon (D; in cm), and soil thickness with carbonate nodules (H in cm). In addition, selected clayey (Bt) horizons were sampled and analyzed by X-ray fluorescence to determine chemical index of alteration without potash ($C = 100\text{-mAl}_2\text{O}_3 / (\text{mAl}_2\text{O}_3 + \text{mCaO} + \text{mMgO} + \text{mNa}_2\text{O})$, where m is moles) and salinization index ($S = (\text{mK}_2\text{O} + \text{mNa}_2\text{O}) / \text{mAl}_2\text{O}_3$, where m is moles). These field and chemical measures are related to mean annual precipitation (P; in mm), seasonality (M; difference between wettest and driest monthly mean in mm), and mean annual temperature (T; in °C), by the following equations derived from large databases for modern soils (Sheldon et al., 2002; Retallack, 2005):

$$P = 137.24 + 6.45D - 0.013D^2, \\ R^2 = 0.52; \quad SE = \pm 147 \text{ mm}; \quad (1)$$

$$P = 221e^{0.0197C}, \\ R^2 = 0.72; \quad SE = \pm 182 \text{ mm}; \quad (2)$$

$$T = -18.5S + 17.3, \\ R^2 = 0.37; \quad SE = \pm 4.4^\circ\text{C}; \quad \text{and} \quad (3)$$

$$M = 0.79H + 13.71, \\ R^2 = 0.58; \quad SE = \pm 22 \text{ mm}. \quad (4)$$

Depth to Bk horizon and paleosol thickness with nodules needs to be adjusted for burial compaction, using standard algorithms (Sheldon and Retallack, 2001) and geological estimates of 800 m of overburden (Woodring, 1957). Paleosols are 79% of their original thickness at this depth of burial, a degree of compaction compatible with observed deformation of rhizoliths (Figs. 5A–D). A correction for greater-than-modern

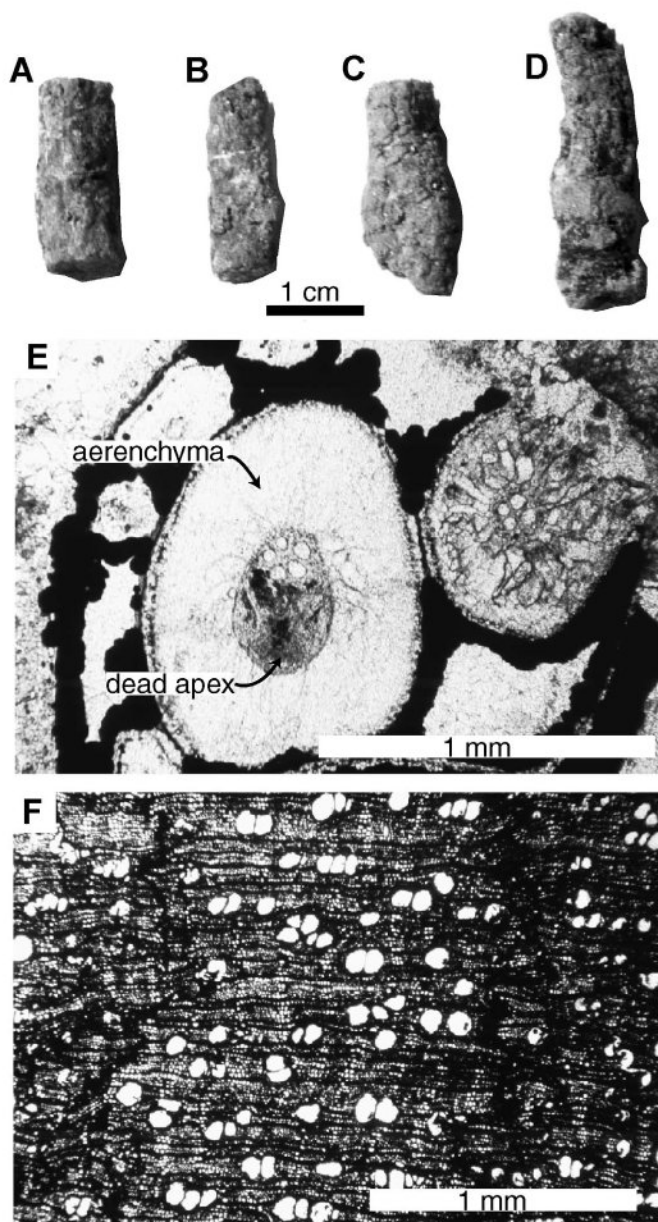


FIGURE 5—Hand specimens (A–D) and petrographic thin section under plane light (E) of rhizoliths interpreted as mangrove peg roots (Condon Collection specimen F40004) from Dote paleosol at 362 m in Puente Centenario section, and ring-porous dicot wood (specimen F40003) in thin section (F) from Paima paleosol at 371 m in Puente Centenario section of the middle Miocene Cucaracha Formation.

atmospheric CO₂ levels was not applied because McFadden and Tinsley (1985) modelled an increase of 2–11 times the present level of atmospheric CO₂ and showed that the depth of pedogenic carbonate increases only by 5 cm. This results in a difference in mean annual precipitation of only 25 mm for a carbonate depth of 50 cm and 18 mm for a carbonate depth of 100 cm; both are well within the standard error of equation (1). Stomatal index studies of fossil *Ginkgo* leaves, as well as other CO₂ paleobarometers, indicate that middle Miocene CO₂ levels no more than 10 times present levels (Retallack, 2002; Demicco et al., 2003).

Climate-sensitive features of the paleosols indicate a middle Miocene mean annual precipitation of 573–916 mm (± 147 mm) based on depth to Bk horizons, with precipitation as much as 1045–1142 mm (± 182 mm) from Bt horizon chemical composition (Fig. 8). Much of the variation within these sections may reflect climatic fluctuation on time scales of tens to hundreds of thousands of years, analogous to interglacial-glacial

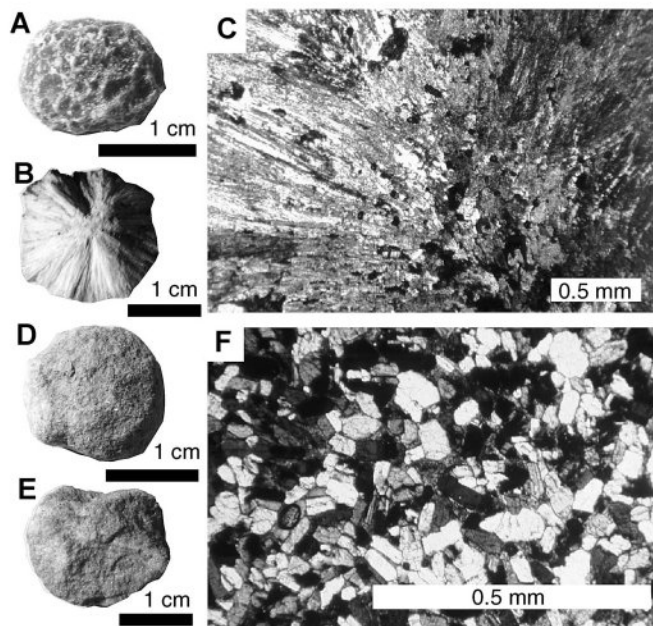


FIGURE 6—Hand specimens and petrographic thin sections viewed under crossed nicols of barite spherulites (A–C) and nodules (D–F) from Kida paleosols at 394 m (Retallack specimen R3195) and 401 m (specimen R3196), respectively, in the Contractors Hill section of the middle Miocene Cucaracha Formation.

(Milankovitch) climatic fluctuations common in paleosols (Retallack et al., 2004); precise periods cannot be assessed without an accurate local time scale from magnetostratigraphy or radiometry. The thickness of profile with carbonate nodules indicates only a 27–65 mm (± 22 mm) difference between the rainiest and driest months. This modest seasonality is supported by the lack of concretionary banding in the paleosol nodules, very weak definition of ring porosity in the fossil wood (Fig. 5F), and lack of seasonal differences in $\delta^{13}\text{C}$ and $\delta^{18}\text{O}$ values in teeth analyzed through annual growth zones (MacFadden and Higgins, 2004). Lack of ruminants in the fossil mammal fauna, unusual for the Miocene, is also compatible with reduced climatic seasonality (Janis et al., 1994; Retallack, 2004b). Mean annual temperature indicated by salinization of Bt horizons was 15–16°C ($\pm 4.4^\circ\text{C}$). This is a warm, temperate, dry climate in the Köppen classification, very different from the wet, seasonally dry, and hot climate of present-day Panama (Fig. 8).

These indications from climate-sensitive paleosol features are supported by identification of comparable modern soils. There are currently no calcareous soils in Panama. The closest calcareous nodular soils in western coastal Venezuela and southeastern Cuba are on sedimentary rock parent materials (Food and Agriculture Organization, 1975). Calcareous soils on volcanoclastic deposits in the rain shadow of the Guatemalan volcanic arc (Weyl, 1980) are most like the Panama middle Miocene paleosols. Calcic Cambisols associated with Vertic Cambisols, Lithosols, and Chromic Luvisols, with inclusions of Pellic and Chromic Vertisols form, an extensive area south of the Motagua River between Hondo and Los Amates, Guatemala (map unit Bk9-3b of Food and Agriculture Organization, 1975). This modern soil landscape is similar to the middle Miocene paleosol assemblage of the Cucaracha Formation (Table 2). Zacapa (425 m), which is within this area, has a mean annual temperature of 26°C and a mean annual precipitation of 653 mm with mean annual range of precipitation of 110 mm (Qwikcast.com, 2006). Nearby Guatemala City is higher (1300 m), to the east of 4000 m volcanic peaks, and has mean annual temperature of 18°C, mean annual precipitation of 1281 mm, and mean annual range of precipitation of 263 mm (Müller, 1982). Both modern weather stations record a greater seasonality of precipitation than is recorded in the paleosols, but these paleosols may be analogues for the extremes of climatic fluctuation seen in the paleosols of the Cucaracha Formation.

TABLE 5—Occurrences of barite nodules in soils and paleosols.

Ma	Age	Formation	Location	Reference
10 ± 6	Miocene or Pliocene	Kuwait Group	Kuwait	Khalaf and El Sayed, 1989
16 ± 1	Barstovian (middle Miocene)	Cucaracha Formation	Gaillard Cut, Panama	Tedford et al., 2004; this paper
16 ± 1	Barstovian (middle Miocene)	Fort Randall Formation	South Bijou Hills, South Dakota, USA	Skinner and Taylor, 1967
18 ± 3	Barstovian-Hemingfordian (early-middle Miocene)	Catahoula Formation	Huntsville, Texas, USA	McKee and Brown, 1977; Patton, 1969; Prothero and Manning, 1987; Wrenn et al. 2003
35 ± 5	Chadronian (late Eocene)	Carroza Formation	La Papa, Mexico	Buck et al. 2003
36 ± 1	Priabonian (late Eocene)	Quasr el Sagha Formation	Fayum Depression, Egypt	Bown and Kraus 1988; Kappelman et al., 1994
45 ± 5	Lutetian (middle Eocene)	Yegua Formation	College Station, Texas, USA	Carson et al., 1982
50 ± 5	Ypresian (early Eocene)	El Naab Formation	Bahariya Oasis, Egypt	Shaalán et al., 1989; Speczik and El Sayed, 1991
90 ± 10	Cenomanian (mid-Cretaceous)	Dunvegan Formation	Clayhurst, British Columbia, Canada	McCarthy and Plint, 2003
90 ± 10	Cenomanian (mid-Cretaceous)	Sabaya Formation	Kharga Oasis, Egypt	Pogue, 1911; Klitzsch, 1978; Hendriks, 1986; El Wahab, 1999; Schrank and Mahmoud, 2000
90 ± 10	Cenomanian (mid-Cretaceous)	Bahariya Formation	Bahariya Oasis, Egypt	Shaalán et al., 1989; Speczik and El Sayed, 1991)
135 ± 5	Berriasian (earliest Cretaceous)	Morrison Formation	Como Bluff, Wyoming	Bakker, 1996; Restallack, personal observations, 2005
151 ± 2	Tithonian (late Jurassic)	Morrison Formation	Thermopolis, Wyoming	Jennings and Hasiotis, 2006a, 2006b
200 ± 5	Hettangian (early Jurassic)	Elliot Formation	Bethlehem, South Africa	Keyser, 1968
250 ± 3	Griesbachian (early Triassic)	Upper Beaufort Group	Thaba Ncha, South Africa	Keyser, 1968
260 ± 2	Guadalupian (middle Permian)	Unidad Roja Superior	Jaca, Spain	Garces and Aguilar, 1994
270 ± 2	Kungurian (early Permian)	Mbuyura Formation	Ruhuhu, Tanzania	Kreuser, 1995
270 ± 2	Kungurian (early Permian)	Garber Sandstone	Norman, Oklahoma, USA	Tarr, 1933; Olson, 1967
270 ± 2	Kungurian (early Permian)	Rotliegend	Rockenberg and Gembeck, Germany	Dietrich, 1975

PALEOVEGETATION

Paleosols of the Cucaracha Formation indicate forest vegetation, in support of palynological (Graham, 1988b) and paleobotanical data (Berry, 1918). Forest is evident from fossil stumps and rhizoliths, as well as from the general profile form of the paleosols, which shows increasingly clayey subsurface (Bt) horizons in better-developed profiles (Restallack, 2001a). The fossil leaves are all entire margined and medium sized (10–15 cm).

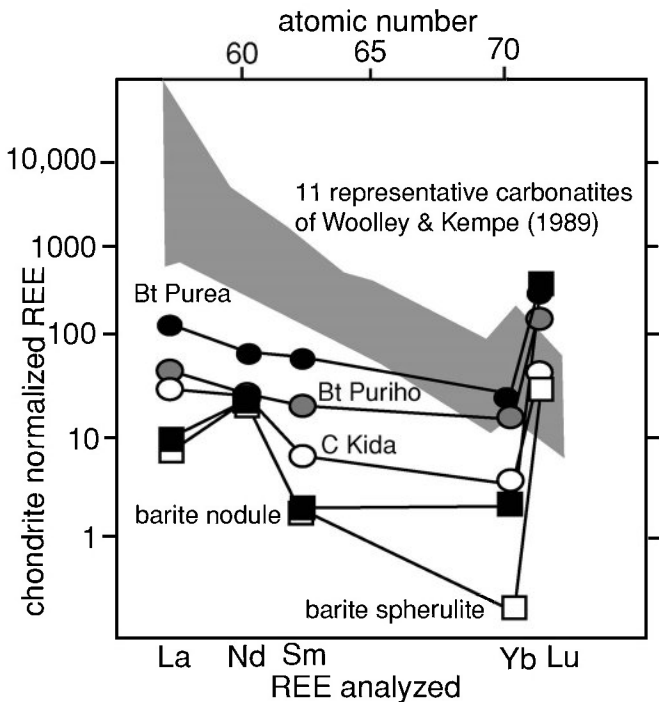


FIGURE 7—Rare earth element analyses of barite nodules and spherulites, their matrix (Kida B horizon), and two associated paleosols (Puraea and Puriho Bt horizons) compared with carbonatite analyses from Woolley and Kempe (1989). REE = rare earth elements.

Berry (1918) did not observe large leaves with drip-tips; nor did we. Fossil stumps and trunks were all smooth barked, as is common for tropical trees. None had the buttress roots that are common in rain forests. None had stringy bark or multiple boles, as is common for dry woodland trees (Restallack, 1991).

Other indications that the flora of the Cucaracha Formation was not rain forest come from the moisture deficit indicated by calcareous nodules in Puriho paleosols and calcareous lower parts of Puraea paleosols. Comparable modern soils support low (<15 m) semievergreen tropical forest like that near Zacapa, Guatemala (Food and Agriculture Organization, 1975). This vegetation may have alternated with medium (15–30 m) evergreen forest during wetter and warmer times, as represented by Puraea paleosols, which are thicker, more clayey, and more deeply weathered than Puriho paleosols.

Paleobotanical evidence of mangrove pollen (Graham, 1988b) and a likely mangrove fern (Berry, 1918) is supported by evidence from pyritic paleosols for both mangrove peat swamps (Itarra pedotype) and mangrove silts (Dote pedotype). Both pedotypes contain rhizoliths interpreted as peg roots that probably belong to *Avicennia*, considering their preserved anatomy (Fig. 5). The Panamanian fossil peg roots lack the taper and thick phelloderm of *Sonneratia* peg roots and the radiating lacunae found in the secondary phloem of *Laguncularia* peg roots (Chapman, 1976). The Panama fossils have stout stellate cells of the aerenchymatous inner cortex, which is more like the New World *Avicennia germinans* than the Old World *A. marina*, which has slender stellate cells (Chapman, 1976). One thin section showed regenerative branching bypassing a dead apex (Fig. 5E), as is commonly found after damage by crabs. A Dote paleosol with peg roots in the uppermost Culebra Formation near Gold Hill (Fig. 3C) is associated with marine clams (*Tellina ophiaca*, *Crassostrea cahobasensis*), snails (*Conus* sp., *Turritella atilira*), crabs (*Euphyllax culebrensis*, *Callinectes declivis*), ghost shrimp (*Callinassa stridens*), and crocodilian scutes (identifications following Rathbun, 1918, 1937; Woodring, 1957, 1982).

Other edaphic vegetation types indicated by paleosols include fresh-water swamp (Paima pedotype), with remains of both palm and dicot wood and leaves. No fossil plants were found in early successional paleosols (Beredeta, Chibigi, Epedeko, and Kida pedotypes) of colonizing forest or in paleosols of sandy littoral woodland (Dume pedotype). These all had woody vegetation,

TABLE 6—Occurrences of gypsum roses in soils and paleosols.

Ma	Age	Formation	Location	Reference
1 ± 1	Quaternary	Unnamed	Great Eastern Desert, Algeria	Travaria-Cros et al., 1971
1 ± 1	Quaternary	Unnamed	Ayn Dar, Saudi Arabia	Al Mohandis, 2002; Al Kofahi et al., 1993
1 ± 1	Quaternary	Unnamed	Chihuahua, Mexico	Lock et al., 1983
1 ± 1	Quaternary	Unnamed	Gamoep, Namaqualand	Keyser, 1968
1 ± 1	Quaternary	Unnamed	Ximong, China	L. Lan, pers. comm., 2004
30 ± 1	mid-Oligocene	Brule Formation	Badlands National Park, South Dakota	Retallack, 1983
34 ± 1	Late Eocene	Jebel Qatrani Formation	Fayum Depression, Egypt	Bown and Kraus, 1988; Kappelman et al., 1994
34 ± 1	Chadronian (late Eocene)	Chadron Formation	Scenic, South Dakota, USA	Retallack, 1983
112 ± 2	Albian (early Cretaceous)	Dequeen Formation	Highland Quarry, Arkansas, USA	Lock, 2002; Lock et al., 1983
249 ± 2	Lystrosaurus zone (early Triassic)	Balfour Formation	Harrismith, Carlton Heights, South Africa	Keyser, 1968; Retallack et al., 2003
253 ± 3	Dicynodon zone (late Permian)	Balfour Formation	Wapadsberg, South Africa	Retallack et al., 2003
254 ± 4	Guadalupian (late Permian)	Shattuck Formation	Rocky Arroyo, New Mexico	Lock, 2002
256 ± 2	Cisticephalus zone (late Permian)	Beaufort Group	Graaf Riet, and Teekloof Pass, South Africa	Keyser, 1968; Smith, 1990
263 ± 5	Tapinocephalus zone (mid-Permian)	Beaufort Group	Graaf Riet, South Africa	Keyser, 1968
280 ± 10	Wolfcampian (early Permian)	Cedar Mesa Formation	Comb Wash, Utah, USA	Lock, 2002

as is clear from the size and surface texture of their rhizoliths. There is no evidence for grasses from pollen (Graham, 1988b) of the Cucaracha Formation, and none of the paleosols shows the fine rhizoliths and crumb ped structure of grassland soils (Retallack, 2004a).

All the fossil mammal teeth we collected came from early successional and open forest paleosols, rather than from paleosols of closed canopy vegetation (Table 3). Kida paleosols representing disturbed, open stream-side habitats yielded remains of small rhinos (*Menoceras barbouri*) and protoceatids (*Paratoceras wardi*). Colonizing forest paleosols (Beredeta and Borobari pedotypes) yielded remains of peccary (*Cynorca* sp.), rhino (*Menoceras barbouri*), and oreodont (*Merycochoerus matthewi*). Otherwise comparable but completely gray paleosols (Chibigi pedotype) yielded no fossils. The best-developed paleosols (Pura and Puriho) are decalcified in their upper portions, so they may not have been sufficiently

alkaline to favor bone preservation (Retallack, 1998). Despite this taphonomic bias, the habitat preferences suggested by these few occurrences are supported by C-isotope analyses of teeth. *Merycochoerus* has the most negative $\delta^{13}\text{C}$ values of -14.6‰ , which is suggestive of more closed canopy than *Paratoceras* with $\delta^{13}\text{C}$ values of -11.3‰ (MacFadden and Higgins, 2004). These data support indications from paleosols of a complex vegetation mosaic (Fig. 9), which is difficult to reconstruct from assemblages of fossil pollen, leaves, and wood without contextual data from paleosols.

Such varied vegetation is well known in Central America today and stimulated Holdridge et al. (1971) to propose a widely cited system of climatic and altitudinal life zones. Low semievergreen forest as envisaged for Puriho paleosols is now dominated by tropical legumes including *Acacia*, *Ateleia*, *Lonchocarpus*, and *Haematoxylon*, whereas medium semievergreen forest as envisaged for Pura paleosols includes such emergent rain-forest trees as the milk tree, *Brosimum* (Food and Agriculture Organization, 1975). Prominent early successional trees in Central America are coyol palm (*Acrocomia*) and umbrella-leaf (*Cecropia*), but other colonizing forest trees include the woody dicots *Cochlospermum*, *Guazuma*, and *Muntingia* (Hartshorn, 1983). Fresh-water swamps are now dominated by large dicots like *Pentaclethra* and *Carapa*, rather than bald cypress characteristic of swamps in northern Mexico and the southeastern United States. Central American mangroves include such woody dicots as *Avicennia*, *Rhizophora*, *Pelliciera*, *Laguncularia*, and *Conocarpus*, rather than salt-marsh grasses of the intertidal zone further north in North America (Chapman, 1976). Strand vegetation includes *Ipomoea*, *Canavalia*, *Hibiscus*, and *Hippomane* (Hartshorn, 1983). These various mangrove, strand, early successional, colonizing, and swamp plants are common in Panama, but the dominant forest cover of Panama today is tall evergreen forest (Leigh, 1999), unlike middle Miocene vegetation (Fig. 9).

PALEOGEOGRAPHIC AND GLOBAL CHANGE IMPLICATIONS

The surprising conclusion of our search for analogous modern soils and vegetation to middle Miocene fossil soils and plants of Panama is that the middle Miocene was quite different from modern conditions: it was drier, cooler, with a less marked dry season, and with more open vegetation of shorter stature (Fig. 9). Comparable soils and vegetation along the Motagua River in Guatemala are at elevations of 425 m in the rain shadow of 4000-m-high volcanoes (Food and Agriculture Organization 1975), but the lower Motagua River is rain forested and much wetter and warmer (mean annual temperature 25.6°C and mean annual precipitation 2587 mm for Tela, Honduras; see Müller, 1982). The Panamanian paleosols were at or near sea level,

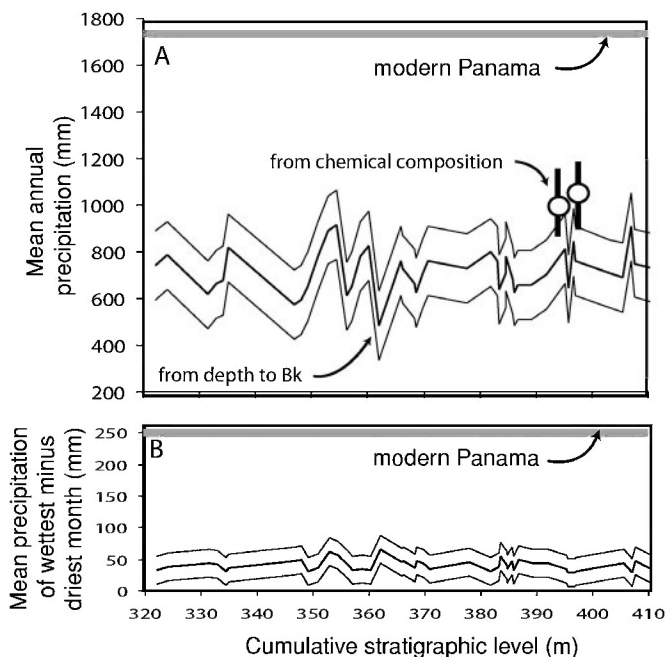
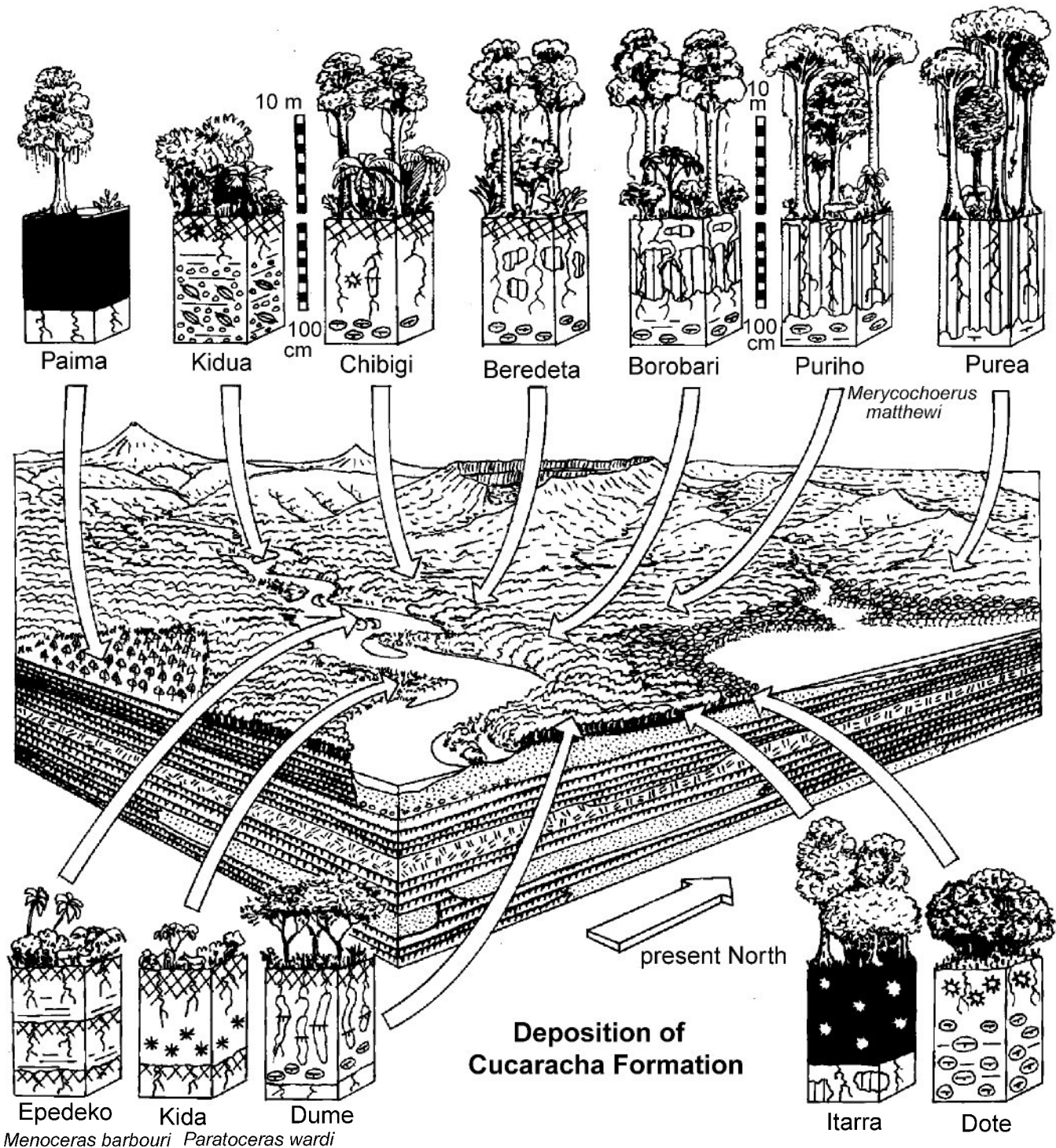


FIGURE 8—Mean annual rainfall and rainfall seasonality inferred from depth and spread of pedogenic carbonate (heavy curves with standard error) and mean annual rainfall inferred from chemical composition of paleosol Bt horizons of paleosols in the Cucaracha Formation.



Menoceras barbouri *Paratoceras wardi*

FIGURE 9—Reconstruction of soils and vegetation of the middle Miocene (Barstovian) Cucaracha Formation, Panama.

as indicated by interbedded mangrove paleosols, so a rain-shadow zone down to sea level would have required a volcanic mountain range of comparable or greater elevation. Such topographic relief is also indicated by fossil pollen of premontane rain forest now found at elevations as much as 1400 m high (Graham, 1982, 1988a, 1988b). This major orographic barrier must also have been geographically extensive because the fossil mammals of the Cucaracha Formation are not only taxonomically identical with North American species but also the same size, rather than different sizes typical for island populations isolated from mainland relatives (Kirby and MacFadden, 2005).

Partial enclosure of the Caribbean by a middle Miocene Panama Pen-

insula to North America (Whitmore and Stewart, 1965; Kirby and MacFadden, 2005), as well as by Antillean volcanic arcs (Iturralde-Vinent and MacPhee, 1999), would have initiated higher Caribbean temperatures and salinities (von der Heydt and Dijkstra, 2005), as was once envisaged for completion of the isthmian barrier during the Pliocene (Broecker, 1989). Caribbean extinctions of corals, bryozoans, and mollusks following cooling of the terminal Oligocene are followed by diversification with middle Miocene warming until Pliocene extinctions (Budd et al., 1996; Cheetham and Jackson, 1996; Jackson et al., 1996; Johnson and Kirby, 2006). Diverse and luxuriant tropical mangal and swamp communities of

the Cucaracha Formation mirror this evolutionary diversification of the Proto-Caribbean marine fauna.

The middle Miocene was a time of dramatic climatic fluctuations, with global temperature and rainfall peaks at 18 and 16 Ma, indicated by $\delta^{18}\text{O}$ values of benthic foraminifera in deep-sea cores (Zachos et al., 2001) and paleosol base loss and desalinization in Oregon (Retallack, 2004b) and Kenya (Retallack, 2007). Barstovian mammals in the Cucaracha Formation suggest correlation of calcareous paleosols with global cooling at about 15 Ma, following peak warmth at 16 Ma for coral reefs and deep marine parts of the middle to upper Culebra Formation. The deep marine part of the upper Culebra Formation (mapped as La Boca Formation until Bold, 1973) has a palynoflora of wet tropical forest including additional mangrove (*Pelliciera*) and wetland plants (*Utricularia*) not found in the lower Culebra and Cucaracha formations (Graham, 1988a). The upper Culebra Formation also lacks dry-forest indicators found in the lower Culebra and Cucaracha formations: *Acacia*, *Crudia*, *Eugenia* or *Myrcia*, Chenopodiaceae-Amaranthaceae, and Compositae (Graham 1988a, 1988b, 1989). The Gaillard Group may represent a climatic cycle of several million years, beginning with moist, medium-height semievergreen forest during the 23–17 Ma deposition of the lower Culebra Formation, then humid, tall semievergreen forest and diverse mangroves with marine transgression for the 16 Ma upper Culebra Formation, followed by dry, low semievergreen forest during 15 Ma accumulation of the continental Cucaracha Formation.

CONCLUSIONS

Our new view of a mountainous (1400–4000 m) peninsula extending all the way from North America to Panama presents a new challenge for climate modeling of middle Miocene climatic oscillations. Such models show that Caribbean enclosure leads to warmer, more saline seawater (von der Heydt and Dijkstra, 2005), and isotopic studies of deep-sea foraminifera suggest global warming at 16 Ma (Zachos et al., 2001). Similarly, final isthmian closure at 3.1–2.8 Ma (Bartoli et al., 2005) coincides with global warming rather than cooling (Zachos et al., 2001). Isthmian constriction and closure coincides with warming, not cooling, yet global cooling at 15 and 2 Ma followed warm spikes at 16 and 3 Ma (Zachos et al., 2001). Such oscillations are evidence against permanent long-term alterations of the world climatic system, like closure of oceanographic gateways (Broecker, 1989), mountain uplift (Raymo and Ruddiman, 1992), or grassland evolution and expansion (Retallack, 2001b).

The Middle Miocene cooling and drying following a warm-humid peak observed in Panama is not entirely due to local mountain building or sea-level change because a similar global climatic cycle is also evident from 15–23 Ma paleosols in Oregon, Montana, Nebraska, Germany, Japan, Kenya, Pakistan, and Australia (Retallack, 1991, 2004b, 2007; Schwarz, 1997). Middle Miocene peaks of heat and humidity with periods of a million years may be due to such short-term perturbations as meteorite impacts (Ries Crater in Germany; Dressler and Reimold, 2001) or flood basalt volcanism (Columbia River Basalts of Oregon; McBirney et al., 1974). Impact and volcanism both produce cooling aerosols and dust followed by CO_2 greenhouse from biomass destruction (Pope et al., 1994). Unusually cool tropical conditions at 15–16 Ma indicated by the Cucaracha Formation paleosols are probably not a transient cooling event but a return to long-term cooling after transient warming, judging from long-term paleoclimatic records outside of Panama (Zachos et al., 2001; Retallack, 2004b, 2007).

ACKNOWLEDGMENTS

MXK thanks the Autoridad del Canal de Panama, especially P. Franceshi, for access to localities and logistical support, and General de Recursos Minerales, especially F.C. de Sierra and J. Villa, for the necessary permits. GJR thanks Egbert Leigh for the invitation and funding to visit Panama. Leah Minc of the Oregon State University Radiation Center

graciously performed rare earth element analyses. Fieldwork was funded by a Smithsonian Institution postdoctoral fellowship to MXK.

REFERENCES

- AL KOFAHI, M.M., HALLAK, A.B., AL JUWAIIR, H.A., and SAAFIN, A.K., 1993, Analysis of desert rose using PIXE and RBS techniques: X-ray Spectrometry, v. 22, p. 23–27.
- AL MOHANDIS, A.A., 2002, Mineralogy and chemistry of desert roses, Ayn Dar area, Abqaiq, eastern province, Saudi Arabia: Qatar University Science Journal, v. 22, p. 191–204.
- ALTSCHULER, Z.S., SCHNEPPE, M.M., SILBER, C.C., and SIMON, F.O., 1983, Sulfur diagenesis in Everglades peat and the origin of pyrite in coal: Science, v. 221, p. 221–227.
- BAKKER, R.T., 1996, The real Jurassic Park: Dinosaurs and habitats at Como Bluff, Wyoming, in Morales, M. ed., The Continental Jurassic: Museum of Northern Arizona Bulletin, v. 60, p. 35–49.
- BARTOLI, G., SARNTHEIN, M., WEINELT, M., ERLKENKEUSER, H., GARBE-SCHÖNBERG, and LEA, D.W., 2005, Final closure of Panama and onset of northern hemisphere glaciation: Earth and Planetary Science Letters, v. 237, p. 33–44.
- BERRY, E.W., 1918, The fossil higher plants from the Canal Zone: Bulletin of the U.S. National Museum, v. 103, 41 p.
- BINDER, R., and ISMARE, C.P., 1997, Vocabulario ilustrado: Wounmeu-Español-Éberä bed'ea: Iglesia Evangelica Unida, Panama City, 174 p.
- BLACUT, G. and KLEINPELL, R.M., 1969, A stratigraphic sequence of benthonic smaller foraminifera from the La Boca Formation, Panama Canal Zone: Cushman Foundation for Foraminiferal Research Contributions, v. 20, p. 1–22.
- BLOW, W.H., 1969, Late middle Eocene to recent planktonic foraminiferal biostratigraphy: First International Conference on Planktonic Microfossils Proceedings, v. 1, p. 199–421.
- BOLD, W. A., VAN DEN, 1973, Ostracoda of the La Boca Formation, Panama Canal Zone: Micropaleontology, v. 18, p. 410–442.
- BOWN, T.M., and KRAUS, M.J., 1988, Geology and paleoenvironment of the Oligocene Jebel Qatrani Formation and adjacent rocks, Fayum Depression, Egypt: U.S. Geological Survey Professional Paper 1452, 60 p.
- BROECKER, W.S., 1989, The salinity contrast between the Atlantic and Pacific Ocean during glacial time: Paleoceanography, v. 4, p. 207–212.
- BUCK, B.J., LAWTON, T.T., MERKLER, D., HAWLEY, R.A., KHRESAT, S., RAWAJFIH, Z., WARDMANN, B., and HANSON, A., 2003, A snowball in the Devils Anus and other adventures in the world of pedogenic sulfates: Geological Society of America Abstracts, v. 35, no. 6, p. 257.
- BUDD, A.F., JOHNSON, K.G., and STEMANN, T.A., 1996, Plio-Pleistocene turnover and extinctions in the Caribbean reef-coral fauna, in Jackson, J.B.C., Budd, A.F., and Coates, A.G., eds., Evolution and Environment in Tropical America: University of Chicago Press, Chicago, p. 168–204.
- CARSON, C.D., FANNING, D.S., and DIXON, J.B., 1982, Alfisols and Ultisols with acid sulfate weathering features in Texas, in Kittrick, J.A., Fanning, D.S., Hossner, L.R., Kral, D.M., and Hawkins, S., eds., Acid Sulfate Weathering: Soil Science Society of America Special Publication 10, p. 127–146.
- CHAPMAN, V.J., 1976, Mangrove Vegetation: J. Cramer, Leutershausen, Germany, 447 p.
- CHEETHAM, A.H., and JACKSON, J.B.C., 1996, Speciation, extinction, and the decline of arboreoscent growth in Neogene and Quaternary cheilostome bryozoa of tropical America, in Jackson, J.B.C., Budd, A.F., and Coates, A.G., eds., Evolution and Environment in Tropical America: University of Chicago Press, Chicago, p. 205–233.
- COATES, A.G., COLLINS, L.S., AUBRY, M.-P., and BERGGREN, W.A., 2004, The geology of the Darien, Panama, and the late Miocene–Pliocene collision of the Panama Arc with northwestern South America: Geological Society of America Bulletin, v. 116, p. 1,327–1,344.
- COATES, A.G., and OBANDO, J.A., 1996, The geologic evolution of the Central American isthmus, in Jackson, J.B.C., Budd, A.F., and Coates, A.G., eds., Evolution and Environment in Tropical America: University of Chicago Press, Chicago, p. 21–26.
- COLEMAN, J.M., 1988, Dynamic changes and processes in the Mississippi River Delta: Geological Society of America Bulletin, v. 100, p. 999–1,015.
- COMPTON, J.J.S., WHITE, R.A., and SMITH, M., 2003, Rare earth element behavior in soil and salt pan sediments of the western Cape, South Africa: Chemical Geology, v. 201, p. 239–255.
- CRONIN, T.M., and DOWSETT, H.J., 1996, Biotic and oceanographic response to the Pliocene closing of the central American Isthmus, in Jackson, J.B.C., Budd, A.F., and Coates, A.G., eds., Evolution and Environment in Tropical America: University of Chicago Press, Chicago, p. 76–104.
- CURRY, R.G., MCCARTNEY, M.S., and JOYCE, T.M., 1998, Oceanic transport of sub-polar climate signals to mid-depth subtropical waters: Nature, v. 391, p. 575–577.
- DARMODY, R.G., HARDING, S.D., and HASSETT, J.J., 1989, Barite authigenesis in sur-

- ficial soils of mid-continental United States, in Miles, D.L., ed., *Water-Rock Interaction: WRI-6*, A.A. Balkema, Rotterdam, p. 183–186.
- DEMICCO, R.V., LOWENSTEIN, T.K., and HARDIE, L.A., 2003, Atmospheric pCO₂ since 60 Ma from records of seawater pH, calcium, and primary carbonate mineralogy: *Geology*, v. 31, p. 793–796.
- DELMELLE, P., and BERNARD, A., 2004, Downstream composition changes of acidic volcanic waters discharged into the Banyupahit Stream, Ijen Caldera, Indonesia: *Journal of Volcanology and Geothermal Research*, v. 97, p. 55–75.
- DICKENS, G.R., FEWLESS, T., THOMAS, T., and BRALOWER, T.J., 2003, Excess barite accumulation during the Paleocene–Eocene thermal maximum: Massive input of dissolved barium from seafloor gas hydrate reservoirs, in Wing, S.L., Gingerich, P.D., Schmitz, B., and Thomas, E., eds., *Causes and consequences of globally warm climates in the early Paleogene*: Geological Society of America Special Paper, v. 369, p. 11–23.
- DIETRICH, M., 1975, *Wüstenrose: Vereinigung der Freunde de Mineralogie und Geologie*, v. 26, p. 217–219.
- DRESSLER, B.D., and REIMOLD, W.J., 2001, Terrestrial impact melt rocks and gasses: *Earth Science Reviews*, v. 56, p. 205–284.
- EL WAHAB, A.A., 1999, Petrography, fabric analysis and diagenetic history of upper Cretaceous sandstones, Kharga Oasis, western desert, Egypt: *Sedimentology of Egypt*, v. 7, p. 99–117.
- FOOD AND AGRICULTURE ORGANIZATION, 1974, *Soil map of the world (Volume I, legend)*: United Nations Educational, Scientific, and Cultural Organization, Paris, 59 p.
- FOOD AND AGRICULTURE ORGANIZATION, 1975, *Soil map of the world (Volume III, Mexico and Central America)*: United Nations Educational, Scientific, and Cultural Organization, Paris, 96 p.
- GARCÉS, B.L.V., and AGUILAR, J.G., 1994, Permian saline lakes in the Aragón-Béarn Basin, western Pyrenees, in Renaut, R.W., and Last, W.M., eds., *Sedimentology and Geochemistry of Modern and Ancient Saline Lakes*: Society for Sedimentary Geology Special Publication, v. 50, p. 267–290.
- GONZÁLEZ-MUÑOZ, M.T., FERNÁNDEZ-LUQUE, B., MARTÍNEZ-RUIZ, F., BEN CHEKROUN, K., ARIAS, J.M., RODRÍGUEZ-GALLEGO, F., MARTÍNEZ-CAÑAMERO, M., and PAYTAN, A., 2003, Precipitation of barite by *Myxococcus xanthus*: possible implications for the biogeochemical cycle of barium: *Applied Environmental Microbiology*, v. 69, p. 5722–5725.
- GOOSENS, P.J., 1969, Soil process for the formation of secondary residual barite deposit in Pascuales (Ecuador, South America): *Convegno Sulla Rimobilizzazione dei Minerali Metallici e Non-metallici Mulas, Cagliari*, v. 1, p. 273–281.
- GRADSTEIN, F.M., OGG, J.G., and SMITH, A.G., 2004, *A Geologic Time Scale 2004*: Cambridge University Press, Cambridge, 589 p.
- GRAHAM, A., 1982, Utilization of the isthmian land bridge during the Cenozoic—Paleobotanical evidence for timing, and the selective influence of altitudes and climate: *Review of Palaeobotany and Palynology*, v. 72, p. 119–128.
- GRAHAM, A., 1988a, Studies in neotropical paleobotany: V. The lower Miocene communities of Panama—The Culebra Formation: *Annals of the Missouri Botanical Garden*, v. 75, p. 1440–1466.
- GRAHAM, A., 1988b, Studies in neotropical paleobotany: VI. The lower Miocene communities of Panama—The Cucaracha Formation: *Annals of the Missouri Botanical Garden*, v. 75, p. 1467–1479.
- GRAHAM, A., 1989, Lower Miocene floras and biogeography of Central America: *Geological Society of Jamaica Journal*, v. 25, p. 8–15.
- HANNEMAN, D.J., and WIDEMAN, C.J., 1991, Sequence stratigraphy of Cenozoic continental rocks, southwestern Montana: *Geological Society of America Bulletin*, v. 103, p. 1335–1345.
- HANOR, J.S., 2000, Barite-celestine geochemistry and environments of formation, in Alpers, C.N., Jambor, J.L., and Nordstrom, D.K., eds., *Sulfate Minerals: Crystallography, geochemistry, and environmental significance: Reviews in Mineralogy and Geochemistry Mineralogical Society of America*, v. 40, p. 193–275.
- HARTSHORN, G.S., 1983, *Plants*, in Janzen, D.H., ed., *Costa Rican Natural History*: University of Chicago Press, Chicago, p. 118–183.
- HENDRIKS, F., 1986, The Maghrabi Formation of the El Kharga area (SW Egypt): Deposits from a mixed estuarine and tidal flat environment of Cenomanian age: *Journal of African Earth Sciences*, v. 5, p. 481–489.
- HOLDRIDGE, L.R., GRENKE, W.C., HATHEWAY, W.H., LIANG, T., and TOSI, J.A., 1971, *Forest Environments in Tropical Life Zones: A Pilot Study*: Pergamon Press, Oxford, 747 p.
- HUSTON, D.L., and LOGAN, G.A., 2004, Barite, BIFs and bugs: Evidence for evolution of the Earth's early hydrosphere: *Earth and Planetary Science Letters*, v. 220, p. 41–55.
- ISELL, R.F., 1996, *The Australian Soil Classification*: Commonwealth Scientific and Industrial Research Organization, Melbourne, 144 p.
- ITURRALDE-VINENT, M.A., and MACPHEE, R.D.E., 1999, Paleogeography of the Caribbean region: Implications for Cenozoic biogeography: *American Museum of Natural History Bulletin*, v. 238, p. 1–95.
- JACKSON, J.B.C., JUNG, P., and FORTUNATO, H., 1996, *Paciphilia revisited: Transisth-*
- mian evolution of the Strombina group (Gastropoda: Columbellidae)*, in Jackson, J.B.C., Budd, A.F., and Coates, A.G., eds., *Evolution and Environment in Tropical America*: University of Chicago Press, Chicago, p. 234–270.
- JANIS, C.M., GORDON, J.J., and ILLUS, A.W., 1994, Modeling equid/ruminant competition in the fossil record: *Historical Biology*, v. 8, p. 15–29.
- JENNINGS, D.S., and HASIOTIS, S.T., 2006a, Taphonomic analysis of a dinosaur feeding site using geographic information systems (GIS), Morrison Formation, southern Bighorn Basin, Wyoming: *PALAIOS*, v. 21, p. 480–492.
- JENNINGS, D.S., and HASIOTIS, S.T., 2006b, Paleoenvironmental stratigraphic implications of authigenic clay distribution in Morrison Formation deposits, Bighorn Basin, Wyoming, USA, in Foster J.R., and Lucas S.G., eds, *Paleontology and geology of the Upper Jurassic Morrison Formation: New Mexico Museum of Science and History Bulletin*, v. 36, p. 25–34.
- JOHNSON, K.G., and KIRBY, M.X., 2006, The Emperor Limestone rediscovered: Early Miocene corals from the Culebra Formation, Panama: *Journal of Paleontology*, v. 80, p. 383–293.
- KAPPELMAN, J., SIMONS, E.L., and SWISHER, C.C., 1994, New age determinations for the Eocene–Oligocene boundary sediments in the Fayum Depression, northern Egypt: *Journal of Geology*, v. 100, p. 647–668.
- KEYSER, A.W., 1968, Some indications of arid climate during the deposition of the Beaufort Series: *Annals Geological Survey of South Africa*, v. 5, p. 77–78.
- KHALAF, H.I., and EL SAYED, M.I., 1989, Occurrence of barite-bearing mud balls within the Mio-Pliocene terrestrial sand (Kuwait Group) in southern Kuwait, Arabian Gulf: *Sedimentary Geology*, v. 64, p. 197–202.
- KIRBY, M.X., and MACFADDEN, B., 2005, Was southern Central America an archipelago or a peninsula in the middle Miocene? A test using land-mammal body size: *Palaeogeography, Palaeoclimatology, Palaeoecology*, v. 228, p. 193–202.
- KLITZSCH, E., 1978, *Geologische Bearbeitung Südwest-Agyptens: Geologische Rundschau*, v. 67, p. 509–520.
- KREUSER, T., 1995, Tectonic and climatic controls of lacustrine sedimentation in pre-rift and rift settings in the Permian–Triassic of East Africa: *Journal of Paleolimnology*, v. 13, p. 3–19.
- KUMP, L.R., PAVLOV, A., and ARTHUR, M., 2005, Massive releases of hydrogen sulfide to the surface ocean and atmosphere during intervals of oceanic anoxia: *Geology*, v. 33, p. 397–407.
- LEAR, C.H., ROSENTHAL, Y., and WRIGHT, J.D., 2003, The closing of a seaway: Ocean water masses and global climate change: *Earth and Planetary Science Letters*, v. 210, p. 425–436.
- LEIGH, E.G., 1999, *Tropical Forest Ecology: A View from Barro Colorado Island*: Oxford University Press, New York, 245 p.
- LEWIS, H.P., 1923, The occurrence of detrital barytes in the Permian basal sand at Nitticarlil: *Geological Magazine*, v. 60, p. 307–313.
- LOCK, B.E., 2002, Sabkhas ancient and modern: *Transactions Gulf Coast Association of Geological Societies*, v. 52, p. 645–657.
- LOCK, B.E., DARLING, B.K., and REX, I.D., 1983, Marginal marine evaporites, lower Cretaceous of Arkansas: *Transactions Gulf Coast Association of Geological Societies*, v. 33, p. 145–152.
- LUND, D.C., LYNCH-STIEGLITZ, J., and CURRY, W.B., 2006, Gulf stream density structure and transport during the past millennium: *Nature*, v. 444, p. 601–604.
- LYNN, W.C., TU, H.Y., and FRANZMEIER, D.P., 1971, Authigenic barite in soils: *Soil Science Society of America Proceedings*, v. 35, p. 160–161.
- MACFADDEN, B.J., 2006, North American Miocene land mammals from Panama: *Journal of Vertebrate Paleontology*, v. 26, p. 720–734.
- MACFADDEN, B.J., and HIGGINS, P., 2004, Ancient ecology of 15-million-year old browsing mammals within C3 communities from Panama: *Oecologia*, v. 140, p. 169–182.
- MACPHERSON, G.L., 1989, Sources of lithium and barium in Gulf of Mexico Basin formation waters, U.S.A., in Miles, D.L., ed., *Water-Rock Interaction: WRI-6*, A.A. Balkema, Rotterdam, p. 453–460.
- MARINCOVICH, L., 2000, Central American paleogeography controlled Pliocene Arctic Ocean molluscan migration: *Geology*, v. 28, p. 551–554.
- MCBIRNEY, A.R., SUTTER, J.F., NASLUND, H.R., SUTTON, K.G., and WHITE, C.M., 1974, Episodic volcanisms in the central Oregon Cascade Range: *Geology*, v. 2, p. 585–589.
- MCCARTHY, P.J., and PLINT, A.G., 2003, Spatial variability of palaeosols across Cretaceous interfluvies in the Dunvegan Formation, NE British Columbia, Canada: *Palaeohydrological, palaeogeomorphological and stratigraphic implications: Sedimentology*, v. 50, p. 1187–1220.
- MCFADDEN, L.D., and TINSLEY, J.L., 1985, Rate and depth of pedogenic carbonate accumulation in soils: Formulation and testing of a compartment model, in Weide, D.L., ed., *Soils and Quaternary Geology of the Southwestern United States: Geological Society of America Special Paper 203*, p. 23–41.
- McKEE, T.R., and BROWN, J.L., 1977, Preparation of specimens for electron microscopic examination, in Dixon, J.B., and Weed, S.B., eds., *Minerals in soil environments: Soil Science Society of America, Madison, Wisconsin*, p. 809–846.
- MEREFIELD, J.R., 1975, Incorporation in soil of barytes derived from mineral veins in southwest England: *Sedimentary Geology*, v. 14, p. 135–148.

- MEITZGER, C.A., TERRY, D.O., and GRANDSTAFF, D.E., 2004, Effect of paleosol formation on rare earth element signatures in fossil bone: *Geology*, v. 30, p. 497–500.
- MÜLLER, M.J., 1982, Selected climatic data for a global set of standard stations for vegetation science: *Junk, The Hague*, 306 p.
- OLSON, E.C., 1967, Early Permian vertebrates of Oklahoma: *Oklahoma Geological Survey Circular*, v. 74, 111 p.
- PATTON, T.H., 1969, Miocene and Pliocene artiodactyls, Texas Gulf Coastal Plain: *Biological Sciences, Florida State Museum Bulletin*, v. 14, p. 115–226.
- PE-PIPER, G., DOLANSKY, L., and PIPER, D.J.W., 2005, Sedimentary environment and diagenesis of the Lower Cretaceous Chaswood Formation, southeastern Canada: The origin of kaolin-rich mudstones: *Sedimentary Geology*, v. 178, p. 75–97.
- POGUE, J.E., 1911, On sand barites from Kharga, Egypt: *U.S. National Museum Proceedings*, v. 38, p. 17–24.
- POPE, K.O., BAINES, K.H., OCAMPO, A.C., and IVANOV, B.A., 1994, Impact winter and the Cretaceous/Tertiary extinctions: Results of a Chicxulub asteroid impact model: *Earth and Planetary Science Letters*, v. 128, p. 719–725.
- PROTHERO, D.R., 2001, Chronostratigraphic calibration of the Pacific Coast Cenozoic: A summary, in Prothero, D.R. ed., *Magnetic stratigraphy of the Pacific Cenozoic: Pacific Section Society of Economic paleontologists and Mineralogists*, Los Angeles, p. 377–394.
- PROTHERO, D.R., and MANNING, E.M., 1987, Miocene rhinoceroses from the Texas Gulf Coastal Plain: *Journal of Paleontology*, v. 61, p. 388–423.
- QWIKCAST.COM, 2006, World Records and Averages, <http://qwikcast.weatherbase.com>. Checked July 9, 2007.
- RATHBUN, M.J., 1918, Decapod crustaceans from the Panama region: *Bulletin of the U.S. National Museum*, v. 103, p. 123–184.
- RATHBUN, M.J., 1937, Cretaceous and Tertiary crabs from Panama and Colombia: *Journal of Paleontology*, v. 11, p. 26–28.
- RAYMO, M.E., and RUDDIMAN, W.F., 1992, Tectonic forcing of late Cenozoic climate: *Nature*, v. 359, p. 112–122.
- RETALLACK, G.J., 1983, Late Eocene and Oligocene paleosols from Badlands National Park, South Dakota: *Geological Society of America Special Paper*, v. 193, 82 p.
- RETALLACK, G.J., 1991, Miocene Paleosols and Ape Habitats in Pakistan and Kenya: *Oxford University Press*, New York, 346 p.
- RETALLACK, G.J., 1998, Fossil soils and completeness of the rock and fossil record, in Donovan, S.K., and Paul, C.R.C., eds., *The adequacy of the fossil record*: Wiley, Chichester, p. 131–162.
- RETALLACK, G.J., 2001a, *Soils of the Past*: Blackwell, Oxford, 404 p.
- RETALLACK, G.J., 2001b, Cenozoic expansion of grasslands and climatic cooling: *Journal of Geology*, v. 109, p. 407–426.
- RETALLACK, G.J., 2002, Carbon dioxide and climate over the past 300 myr: *Royal Society of London Philosophical Transactions*, ser. B, v. 360, p. 659–673.
- RETALLACK, G.J., 2004a, Late Oligocene bunch grasslands and early Miocene sod grasslands from central Oregon: *Palaeogeography Palaeoclimatology Palaeoecology*, v. 207, p. 203–237.
- RETALLACK, G.J., 2004b, Late Miocene climate and life on land in Oregon within a context of Neogene global change: *Palaeogeography, Palaeoclimatology, Palaeoecology*, v. 214, p. 97–123.
- RETALLACK, G.J., 2005, Pedogenic carbonate proxies of amount and seasonality of precipitation: *Geology*, v. 33, p. 333–336.
- RETALLACK, G. J., 2007, Paleosol, in Henke, W., and Tattersall, I., K.K., eds., *Handbook of Paleoanthropology (Volume 1, Principles, Methods and Approaches)*: Springer, Berlin, p. 383–408.
- RETALLACK, G.J., BESTLAND, E.A., and FREMD, T.J., 2000, Eocene and Oligocene paleosols of central Oregon: *Geological Society of America Special Paper*, v. 344, p. 1–192.
- RETALLACK, G.J., SMITH, R.M.H., and WARD, P.D., 2003, Vertebrate extinction across the Permian–Triassic boundary in the Karoo Basin, South Africa: *Geological Society of America Bulletin*, v. 115, p. 1,133–1,152.
- RETALLACK, G.J., WYNN, J.G., and FREMD, T.J., 2004, Glacial-interglacial-scale paleoclimatic changes without large ice sheets in the Oligocene of central Oregon: *Geology*, v. 32, p. 297–300.
- ROBINSON, W.O., WHETSTONE, R.R., and BYERS, H.G., 1939, Studies on infertile soils, pt. 2: Soils high in barium: *Soil Science Society of America Proceedings*, v. 3, p. 87–91.
- SCHRANK, E., and MAHMOUD, M.S., 2000, New taxa of angiosperm pollen and associated palynomorphs from the early late Cretaceous of Egypt (Mahrabi Formation, Kharga Oasis): *Review of Palaeobotany and Palynology*, v. 112, p. 167–188.
- SCHULTZ, C.B., and STOUT, T.M., 1980, Ancient soils and climatic changes in the central Great Plains: *Nebraska Academy of Sciences Transactions*, v. 8, p. 187–205.
- SCHWARZ, T., 1997, Lateritic paleosols in central Germany and implications for Miocene paleoclimates: *Palaeogeography, Palaeoclimatology, Palaeoecology*, v. 129, p. 37–50.
- SHAALAN, M.M.B., EL ANBAAWY, M.I.H., KOLKILA, A.A., and ALI, M.M., 1989, On the barite deposits of Bahariya Oases, Egypt: *Archiwum Mineralogiczne*, v. 44, p. 21–35.
- SHACKLETTE, H.T., and BOERNGEN, J.G., 1984, Element concentrations in soils and other surficial materials of the conterminous United States: *U.S. Geological Survey Professional Paper 1,270*, 105 p.
- SHELDON, N.D., and RETALLACK, G.J., 2001, Equation for compaction of paleosols due to burial: *Geology*, v. 29, p. 247–250.
- SHELDON, N.D., and RETALLACK, G.J., 2002, Low oxygen levels in earliest Triassic soils: *Geology*, v. 30, p. 919–922.
- SHELDON, N.D., RETALLACK, G.J., and TANAKA, S., 2002, Geochemical climofunctions from North American soils and application to paleosols across the Eocene–Oligocene boundary in Oregon: *Journal of Geology*, v. 110, p. 687–696.
- SKINNER, M.F., and TAYLOR, B.E., 1967, A revision of the geology and paleontology of the Bijou Hills, South Dakota: *American Museum Novitates* 2,300, 53 p.
- SMITH, R.M.H., 1990, Alluvial paleosols and pedofacies sequences in the Permian Lower Beaufort of the southwestern Karoo Basin, South Africa: *Journal of Sedimentary Petrology*, v. 60, p. 155–170.
- SOIL SURVEY STAFF, 1999, *Keys to soil taxonomy*: Pocahontas Press, Blacksburg, Virginia, 600 p.
- SPECZIK, S., and EL SAYED, A.A.Y., 1991, Fluid inclusion studies of Bahariya barites (Western Desert, Egypt): *Acta Geologica Polonica*, v. 41, p. 109–116.
- STOOPS, G.J., and ZAVALETA, A., 1978, Micromorphological evidence of barite neoformation in soils: *Geoderma*, v. 20, p. 63–70.
- TARR, W.A., 1933, The origin of the sand barites of the lower Permian of Oklahoma: *American Mineralogist*, v. 18, p. 260–272.
- TEDFORD, R.H., ALBRIGHT, L.B., BARNOSKY, A.D., FERRUSQUIA-VILLAFRANCA, I., HUNT, R.M., STORER, J.E., SWISHER, C.C., VOORHIES, M.R., WEBB, S.D., and WHISTLER, D.P., 2004, Mammalian biochronology of the Arikaraean through Hemphillian interval (late Oligocene through early Pliocene epochs), in Woodburne, M.O., ed., *Late Cretaceous and Cenozoic Mammals of North America*: Columbia University Press, New York, 169–231.
- TERANES, J.L., GEARY, D.H., and BEMIS, B.E., 1996, The oxygen isotopic record of seasonality in Neogene bivalves from the Central American Isthmus, in Jackson, J.B.C., Budd, A.F., and Coates, A.G., eds., *Evolution and Environment in Tropical America*: University of Chicago Press, Chicago, p. 105–129.
- TORNABENE, L.L., STEWART, R.H., and RYAN, J.G., 1999, Characterization and age of a probable Tertiary impact site near Gamboa, Panama Canal Zone: *Geological Society of America Abstracts*, v. 31, no. 7, p. 174.
- TORRES, M.E., BRUMSACK, H.J., BOHRMANN, G., and EMEIS, K.C., 1996, Barite fronts in continental margin sediments: A new look at barium remobilization in the zone of sulfate reduction and formation of heavy barites in diagenetic fronts: *Chemical Geology*, v. 127, p. 125–129.
- TRAVERÍA-CROS, A., AMIGÓ, J.M., and MONTORIOL-POUS, J., 1971, Nota sobre una masa de “rosas del desierto” reconocida en el Gran Erg oriental (Argelia): *Acta Geologica Hispanica*, v. 6, p. 49–52.
- VON DER HEYDT, A., and DIJKSTRA, H.A., 2005, Flow reorganizations in the Panama Seaway: A cause for the demise of Miocene corals? *Geophysical Research Letters*, v. 32, no. 2, 4 p. : DOI: 10.1029/2004GL020990.
- WEBB, S.D., and RANCY, A., 1996, Late Cenozoic evolution of the Neotropical mammal fauna, in Jackson, J.B.C., Budd, A.F., and Coates, A.G., eds., *Evolution and Environment in Tropical America*: University of Chicago Press, Chicago, p. 335–358.
- WEYL, R., 1980, *Geology of Central America*: Gebrüder Borntraeger, Berlin, 371 p.
- WHITMORE, F.C., and STEWART, R.H., 1965, Miocene mammals and Central American seaways: *Science*, v. 148, p. 180–185.
- WOODRING, W.P., 1957, Geology and description of Tertiary mollusks (gastropods; Trochidae to Turritellidae), Geology and paleontology of Canal Zone and adjoining parts of Panama: *U.S. Geological Survey Professional Paper 306A*, 145 p.
- WOODRING, W.P., 1982, Geology and paleontology of Canal Zone and adjoining parts of Panama; description of Tertiary mollusks: Pelecypods, Propeamussiidae to Cuspidariidae; additions to families covered in P306-E; additions to gastropods; cephalopods: *U.S. Geological Survey Professional Paper*, v. 306F, p. 541–759.
- WOOLLEY, A.R., and KEMPE, D.R.C., 1989, Carbonatites: Nomenclature, average chemical compositions and element distribution, in Bell, K., ed., *Carbonatites*: Unwin Hyman, London, p. 1–14.
- WRENN, J.H., ELSIK, W.C., and MCCULLOCH, R.P., 2003, Age and environments of the Catahoula Formation outcrops in Big Creek, Sicily Island, Catahoula Parish, Louisiana: *Abstracts Geological Society of America*, v. 35, no. 1, p. 18.
- ZACHOS, J., PAGANI, M., SLOAN, L., THOMAS, E., and BILLUPS, K., 2001, Trends, rhythms, and aberrations in global climate 65 Ma to present: *Science*, v. 292, p. 686–693.